ANNEX 5: FAN MODEL

5.1. Fan model flow-pressure laws

The fan flow-pressure laws are defined from the following inputs:

- The total pressure drop delivered by the fan Δp_{total}
- The fan total volume air flow $\dot{V}$
- The fan diameter D

The flow-pressure laws include ϕ, ψ and λ as no dimensional parameters:

$$\phi = \alpha_0 + \alpha_1 \cdot \psi + \alpha_2 \cdot \psi^2 + \alpha_3 \cdot \psi^3$$
$$\lambda = \beta_0 + \beta_1 \cdot \psi + \beta_2 \cdot \psi^2 + \beta_3 \cdot \psi^3 \qquad \text{(A 5.1)}$$

The flow factor ϕ is defined from the reference area A and the peripheral speed U:

$$\phi = \frac{\dot{V}}{A \cdot U} \qquad A = \pi \cdot \frac{D^2}{4}$$
$$U = \pi \cdot D \cdot N \qquad N = \frac{rpm}{60} \qquad \text{(A 5.2)}$$

The pressure factor ψ is defined from the static pressure, from the exhaust dynamic pressure and from the peripheral dynamic pressure (v is the air specific volume defined at fan supply and A_{ex} is the fan exhaust area):

$$\psi = \frac{\Delta P_{total}}{P_{dynam,periph}} \qquad \Delta P_{total} = \Delta P_{stat} + P_{dynam,ex}$$
$$P_{dynam,ex} = \frac{C_{ex}^{\,2}}{2 \cdot v} \qquad C_{ex} = \frac{\dot{V}}{A_{ex}} \qquad \text{(A 5.3)}$$
$$P_{dynam,periph} = \frac{U^2}{2 \cdot v}$$

The power factor λ is related to the isentropic effectiveness ε_s (ratio of the fan isentropic power to the shaft power):

$$\lambda = \frac{\phi \cdot \psi}{\varepsilon_s}$$
$$\varepsilon_s = \frac{\dot{W}_s}{\dot{W}_{shaft}} \qquad \dot{W}_s = \dot{V} \cdot \Delta P_{total} \qquad \text{(A 5.4)}$$

The coefficients α_i and β_i are computed by a regression analysis for both supply/return fans and for an exhaust fan.

5.2. Free cooling exhaust fan regression law

A regression is performed on Soler-Palau exhaust fan TCDV2 040 TCDH2 040 curves, on the basis of the following data:

rpm = 1500 [t/min]   D = 0.54 [m]

Air flow m^3/h	Δp_{stat} *Pa*
1500	405
2000	390
2500	380
3000	360
3500	337
4000	300
4500	237

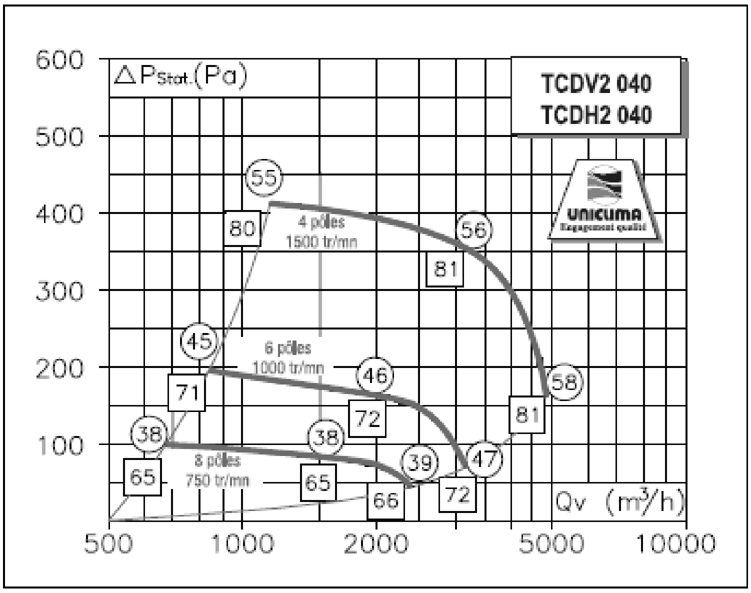

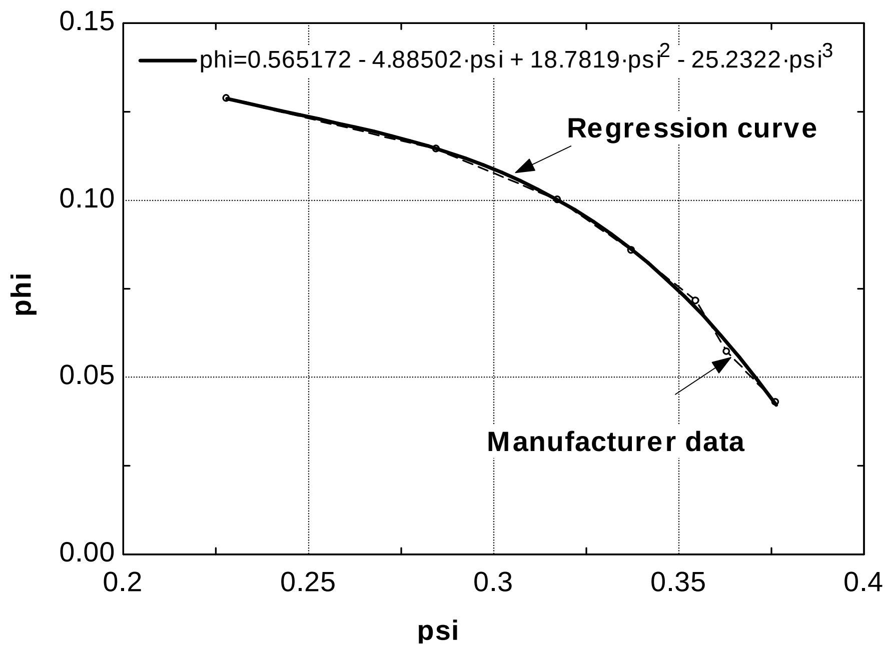

Fig A5.1: Regression curve corresponding to Soler-Palau exhaust fan TCDV2 040 TCDH2 040

The following regression law is obtained, where ψ is computed from the Δp_{tot}:

$$\phi = 0.5652 - 4.885 \cdot \psi + 18.78 \cdot \psi^2 - 25.232209 \cdot \psi^3$$

With a regression coefficient $R^2=99.8$ %. The dynamic pressure is computed from an exhaust air speed calculated trough an exhaust cylindrical area of diameter D and height equal to 0.35.D. The fan efficiency is considered as constant and equal to e = 0.6.

5.3. AHU supply and return fan regression laws

Two regressions were performed on Soler-Palau CVTT-12/12 fan, on the basis of the following data:

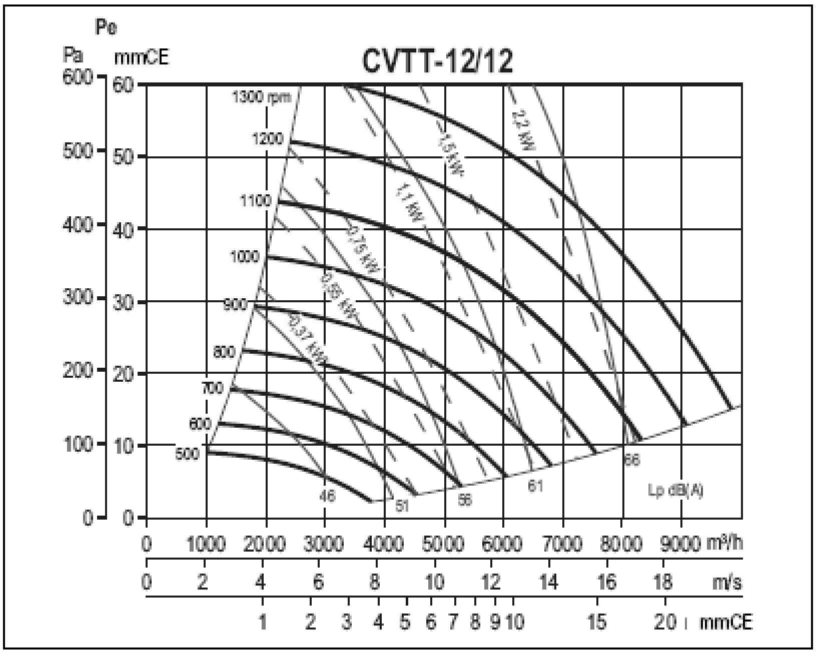

rpm = 1000 [t/min]

D = 0.3048 [m]

Air flow m^3/h	Δp_{stat} *Pa*	Δp_{dyn} *Pa*	W_{el} *W*
2000	353	10	442
3000	343	25	560
4000	319	39	745
5000	280	64	966
6000	221	91	1230
7000	142	123	1510

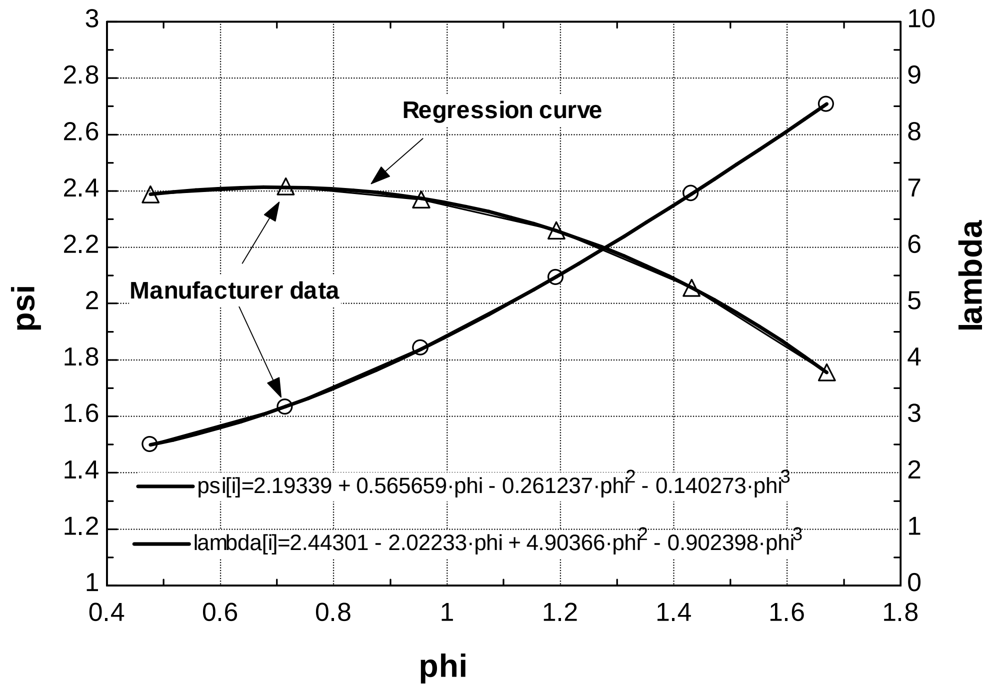

Fig A5.2: Regression curve corresponding to Soler-Palau CVTT-12/12 fan

The following regression laws are obtained, where ψ is computed from the Δp_{tot}:

$$\psi = 2.193 + 0.5657 \cdot \phi - 0.2612 \cdot \phi^2 - 0.1403 \cdot \phi^3$$

With a regression coefficient $R^2=99.99\ \%$.

$$\lambda = 2.443 - 2.0223334 \cdot \phi + 4.904 \cdot \phi^2 - 0.9024 \cdot \phi^3$$

With a regression coefficient $R^2=100\ \%$.

ANNEX 6: VENTILATION MODELS

6.1. House ventilation model

6.1.1 Natural ventilation model

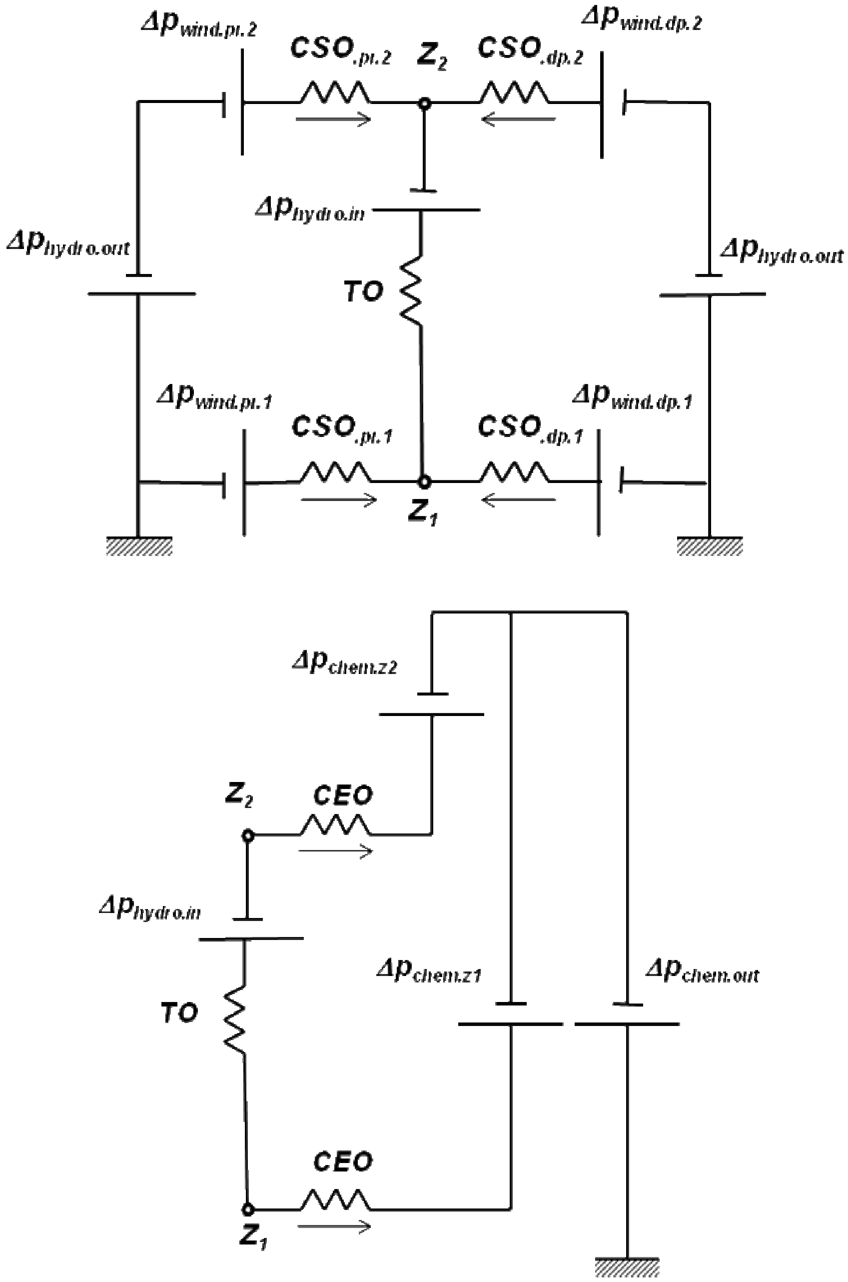

Fig. A 6.1 House natural ventilation model including two zones.

The model can include external Controlled Supply Orifices and Transfer Orifice from one zone to the other (fig. A 6.1 up). It can also include the grid pressure loss from each zone to its exhaust vertical duct and from the exhaust duct to the outdoor, through a global Controlled Exhaust Orifice *K* coefficient (fig. A 6.1 down).

House natural ventilation model can be translated trough the following equations regarding pressure equilibrium and air flows balance:

Pressure drops through pressurized (or depressurized) Controlled Supply Orifices:

$$\begin{aligned}
\Delta p_{pr} &= K_{cso,pr} \cdot \dot{M}_{cso,pr} \cdot \left|\dot{M}_{cso,pr}\right|^{n_{CSO}} \\
\Delta p_{dp} &= K_{cso,dp} \cdot \dot{M}_{cso,dp} \cdot \left|\dot{M}_{cso,dp}\right|^{n_{CSO}} \\
\Delta p_{CEO} &= K_{ceo} \cdot \dot{M}_{CEO} \cdot \left|\dot{M}_{CEO}\right|^{n_{CEO}} \\
\Delta p_{chem} &= K_{chem} \cdot \dot{M}_{CEO} \cdot \left|\dot{M}_{CEO}\right|^{n_{CEO}} \\
\Delta p_{TO} &= K_{cto,z1z2} \cdot \dot{M}_{z1z2} \cdot \left|\dot{M}_{z1z2}\right|^{n_{CTO}}
\end{aligned} \qquad \text{(A6.1)}$$

Pressure equilibrium:

Ring 1: wind pressurized and wind depressurized CSO (controlled air supply orifices)

$$\begin{aligned}
-\Delta p_{wind,dp,1} + \Delta p_{cso,dp,1} - \Delta p_{cso,pr,1} + \Delta p_{wind,pr,1} &= 0 \\
-\Delta p_{wind,dp,2} + \Delta p_{cso,dp,2} - \Delta p_{cso,pr,2} + \Delta p_{wind,pr,2} &= 0
\end{aligned} \qquad \text{(A6.2)}$$

Ring 2: CEO (controlled air exhaust orifices) and air exhaust chimneys:

$$\Delta p_{chem,out} + \Delta p_{chem,1} - \Delta p_{chem,z1} + \Delta p_{CEO,1} - \Delta p_{cso,pr,1} + \Delta p_{wind,pr,1} = 0$$

$$\Delta p_{chem,out} + \Delta p_{chem,2} - \Delta p_{chem,z2} + \Delta p_{CEO,2} - \Delta p_{cso,pr,2} + \Delta p_{wind,pr,2} - \Delta p_{hydro,out} = 0$$

Ring 3: wind pressurized CSO and transfer orifices (TO):

$$-\Delta p_{wind,pr,1} + \Delta p_{cso,pr,1} + \Delta p_{TO} + \Delta p_{hydro,in} - \Delta p_{cso,pr,2} + \Delta p_{wind,pr,2} - \Delta p_{hydro,out} = 0$$

Mass air flow rate balance:

$$\begin{aligned}
\dot{M}_{cso,pr,1} + \dot{M}_{cso,dp,1} + \dot{M}_{CEO,1} &= \dot{M}_{z1z2} \\
\dot{M}_{cso,pr,2} + \dot{M}_{cso,dp,2} + \dot{M}_{CEO,2} &= -\dot{M}_{z1z2}
\end{aligned} \qquad \text{(A6.3)}$$

6.1.2. Window stack effect

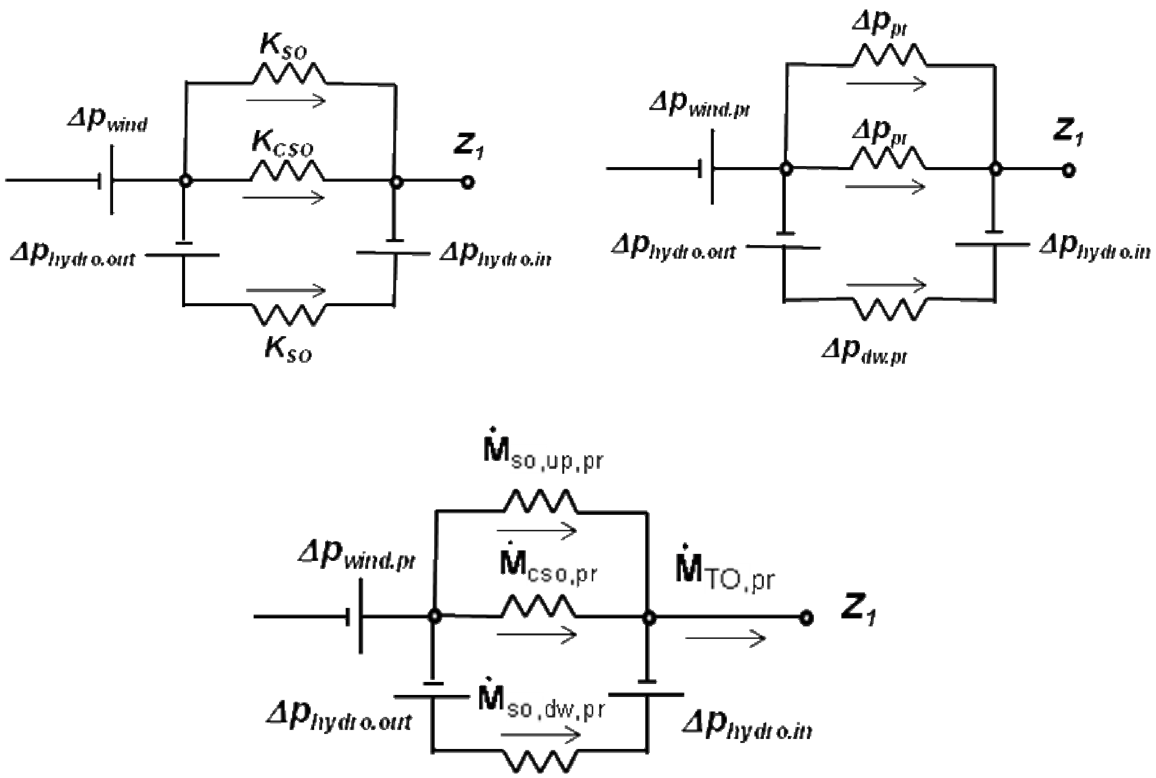

Fig. A 6.2: Model of window stack effect coupled with Controlled Supply Orifices

The K coefficient of a half window or half leakage area is computed from the corresponding coefficients of the whole areas:

$$K_{h,wd} = 2^{n_{wd}+1} . K_{wd} \qquad\qquad K_{h,leak} = 2^{n_{leak}+1} . K_{leak}$$

K_{SO} coefficient and n_{SO} exponent are either data related to a half window when the window is opened, or to the wall half leakage area when the window is closed:

$$n_{SO} = (1 - f_{open,window}) \cdot n_{leak} + f_{open,window} \cdot n_{wd}$$
$$K_{so} = (1 - f_{open,window}) \cdot K_{hleak} + f_{open,window} \cdot K_{hwd} \qquad \text{(A 6.4)}$$

Equations (A 6.4) and (A 6.5) are added to account for the windows stack effect joined to each pressurized CSO resistance (fig. A 6.1). Similar equations are added for the depressurized windows.

Pressure drops:

$$\Delta p_{pr} = K_{so} \cdot \dot{M}_{so,up,pr} \cdot \left|\dot{M}_{so,up,pr}\right|^{n_{exp,SO}}$$

$$\Delta p_{dw,pr} = K_{so} \cdot \dot{M}_{so,dw,pr} \cdot \left|\dot{M}_{so,dw,pr}\right|^{n_{exp,SO}}$$

Pressure equilibrium inside the zones:

$$\Delta p_{pr} - \Delta p_{hydro,wd,in} - \Delta p_{dw,pr} + \Delta p_{hydro,wd,out} = 0 \qquad \text{(A 6.5)}$$

Mass air flow rate balance:

$$\dot{M}_{cso,pr,1} + \dot{M}_{so,up,pr,1} + \dot{M}_{so,dw,pr,1} + \dot{M}_{cso,dp,1} + \dot{M}_{so,up,dp,1} + \dot{M}_{so,dw,dp,1} + \dot{M}_{CEO,1} = \dot{M}_{z1z2}$$

$$\dot{M}_{cso,pr,2} + \dot{M}_{so,up,pr,2} + \dot{M}_{so,dw,pr,2} + \dot{M}_{cso,dp,2} + \dot{M}_{so,up,dp,2} + \dot{M}_{so,dw,dp,2} + \dot{M}_{CEO,2} = -\dot{M}_{z1z2}$$

6.1.3 Combined natural and fan powered ventilation

The house natural ventilation model of fig. A6.1 can be adapted to deal with fan powered air flows through imposed fan air flows (fig. A 6.3).

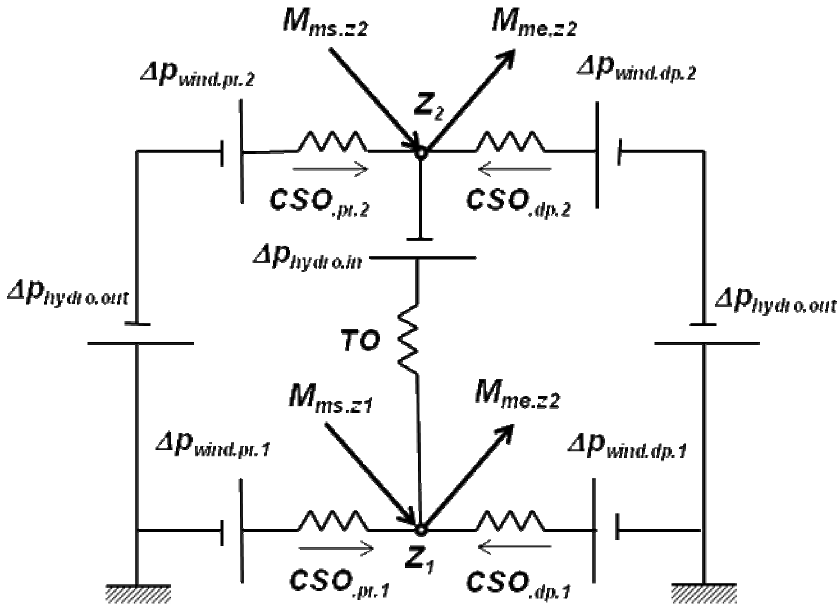

Fig. A 6.3 Model of house combined natural/mechanical ventilation including two zones provided with imposed supply and exhaust fans air flows. The model above must be completed with the exhaust chimney branch represented on fig. A 6.1 down.

Mass air flow rate balance (equation A 6.3) can be modified as follows to include fans air flows:

$$\dot{M}_{nat,1} = \dot{M}_{cso,pr,1} + \dot{M}_{so,up,pr,1} + \dot{M}_{so,dw,pr,1} + \dot{M}_{cso,dp,1} + \dot{M}_{so,up,dp,1} + \dot{M}_{so,dw,dp,1} + \dot{M}_{CEO,1}$$

$$\dot{M}_{nat,2} = \dot{M}_{cso,pr,2} + \dot{M}_{so,up,pr,2} + \dot{M}_{so,dw,pr,2} + \dot{M}_{cso,dp,2} + \dot{M}_{so,up,dp,2} + \dot{M}_{so,dw,dp,2} + \dot{M}_{CEO,2}$$

$$\dot{M}_{nat,1} + \dot{M}_{MS,1} + \dot{M}_{ME,1} = \dot{M}_{z1z2} \qquad \text{(A 6.6)}$$

$$\dot{M}_{nat,2} + \dot{M}_{MS,2} + \dot{M}_{ME,2} = -\dot{M}_{z1z2}$$

6.2. Office building ventilation model

6.2.1. Natural ventilation model

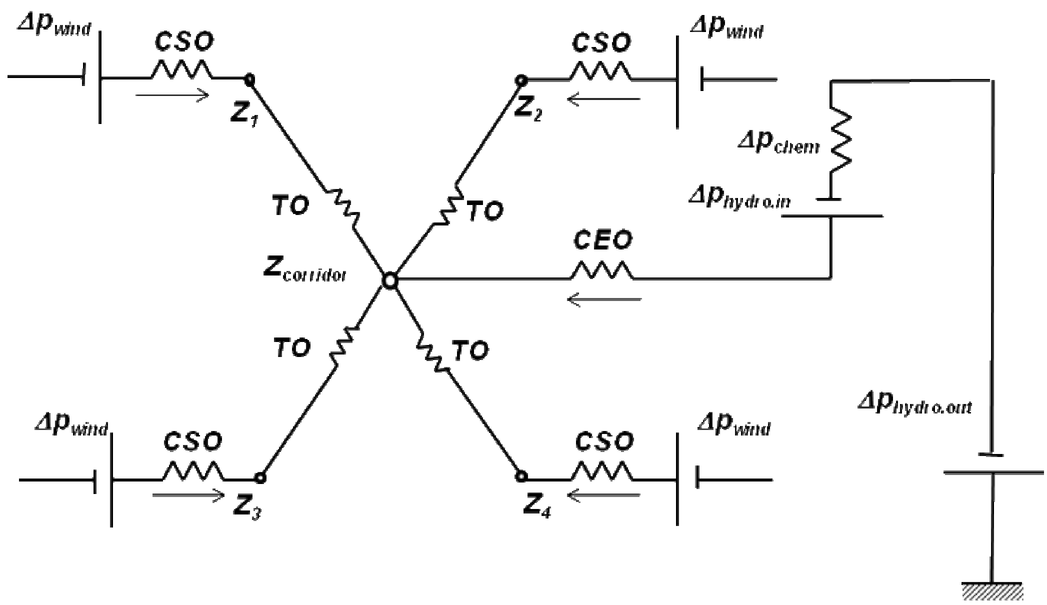

Fig. A 6.4 Natural ventilation model including four zones and a corridor connected to a stack effect from the corridor to a staircase, elevator shaft or ventilation shaft.

Equations related to the house two zones model are adapted for the four office zones model, the zones being all considered as conventionally pressurized and provided with windows stack effects (fig. A 6.4):

Pressure drops:

For each zone:

$$\Delta p_{pr} = K_{cso} \cdot \dot{M}_{cso} \cdot \left|\dot{M}_{cso}\right|^{n_{CSO}}$$

$$\Delta p_{pr} = K_{so} \cdot \dot{M}_{so,up} \cdot \left|\dot{M}_{so,up}\right|^{n_{SO}} \qquad \text{(A 6.7)}$$

$$\Delta p_{pr,dw} = K_{so} \cdot \dot{M}_{so,dw} \cdot \left|\dot{M}_{so,dw}\right|^{n_{SO}}$$

$$\Delta p_{TO} = K_{cto} \cdot \dot{M}_{TO} \cdot \left|\dot{M}_{TO}\right|^{n_{CTO}}$$

For the corridor:

$$\Delta p_{CEO} = K_{ceo} \cdot \dot{M}_{CEO} \cdot \left|\dot{M}_{CEO}\right|^{n_{CEO}}$$

$$\Delta p_{chem} = K_{chem} \cdot \dot{M}_{CEO} \cdot \left| \dot{M}_{CEO} \right|^{n_{CEO}}$$

Pressure equilibrium:

For each zone:

$$-\Delta p_{wind,pr} + \Delta p_{pr} + \Delta p_{TO} - \Delta p_{CEO} + \Delta p_{hydro,in} - \Delta p_{chem} - \Delta p_{hydro,out} = 0$$

$$\Delta p_{pr} - \Delta p_{hydro,wd,in} - \Delta p_{dw,pr} + \Delta p_{hydro,wd,out} = 0 \qquad \text{(A 6.8)}$$

Mass air flow rate balance:

For each zone:

$$\dot{M}_{TO} = \dot{M}_{cso} + \dot{M}_{so,up} + \dot{M}_{so,dw} \qquad \text{(A 6.9)}$$

For the corridor:

$$\dot{M}_{CEO} + \sum_{j=1}^{n_{zones}} (\dot{M}_{TO}) = 0$$

6.2.2. Combined natural and fan powered ventilation

Systems C and D are mainly encountered in office buildings (fig. A6.5):

- C: natural air supply through Controlled Supply Orifices, natural air transfer through Transfer Orifices and fan powered air exhaust.
- D: fan powered air supply, air transfer through Transfer Orifices and fan powered air exhaust, with possible air heat recovery.

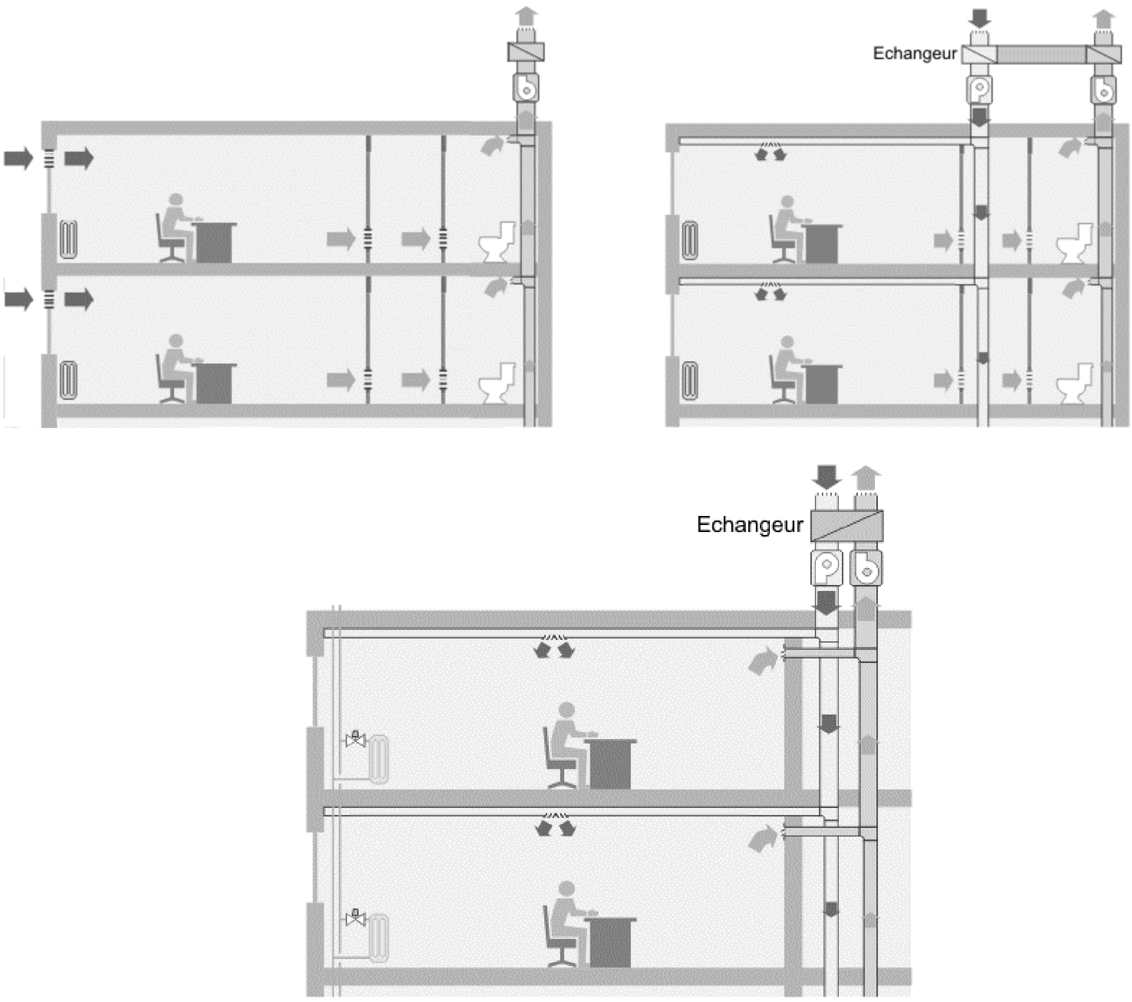

Fig. A 6.5 Office ventilation systems: type C (up left), and D (up right and down) [39].

6.2.2.1. Type C ventilation in office buildings

Type C system can be easily modelled on fig. A 6.6 scheme, which is similar to the natural ventilation scheme of fig. A 6.4, with an exhaust fan added to the exhaust shaft. The building zones are connected to the corridor through transfer orifices.

When the model is used for hygienic air renewal purpose, the corridor can be connected to a ventilation shaft through a grid aperture. An exhaust fan can be located on top of the vertical air duct, working during building occupancy. Equations (A 6.7) to (A 6.9) are modified to model type C system.

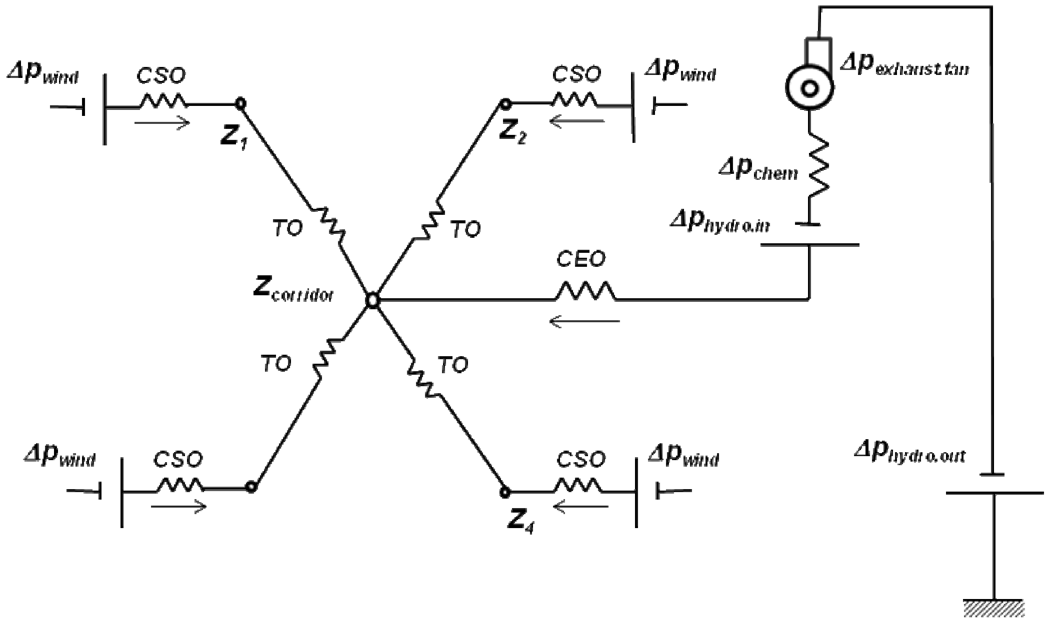

Fig.A 6.6 Type C combined ventilation model including four zones and a corridor connected to an exhaust fan.

Pressure balance for each zone:

$$\Delta p_{out,cor} = -\Delta p_{wind,pr} + \Delta p_{pr} + \Delta p_{TO}$$
$$\Delta p_{cor,out} = -\Delta p_{CEO} + \Delta p_{hydro,in} - \Delta p_{chem} - \Delta P_{stat,exhaustfan} - \Delta p_{hydro,out}$$
$$\Delta p_{out,cor} + \Delta p_{cor,out} = 0 \qquad \text{(A 6.10)}$$
$$\Delta p_{pr} - \Delta p_{hydro,wd,in} - \Delta p_{dw,pr} + \Delta p_{hydro,wd,out} = 0$$

Mass air flow rate balance for the corridor:

$$\dot{M}_{CEO} + \sum_{j=1}^{n_{zones}} (\dot{M}_{TO,j}) = 0$$
$$\dot{M}_{a,exhaustfan} = -n_{wings} \cdot \dot{M}_{CEO} \qquad \text{(A 6.11)}$$

$\dot{M}_{CEO} > 0$ when the air is entering from the outdoor to the corridor while $\dot{M}_{a,exhaustfan} > 0$ when the air is leaving the corridor to the outdoor.

n_{wings} is the number of identical four offices areas in the whole building, all of them being delivered with the same exhaust fan.

When the model is used for free-cooling, the corridor can be connected to a specific ventilation shaft at each building floor, through a grid aperture. An exhaust fan is located on the roof to perform free-cooling during the night with opened windows and doors. Each floor is provided with its own free-cooling exhaust fan, which is sized to reach an air renewal rate of 6 h^{-1} in the offices.

6.2.2.2. Type D ventilation in office buildings

Type D system includes two air ducts networks: one supplying air to the offices and one returning it from the offices to the outdoor (fig. A 6.5). Modelling the system implies not only to model the supply and return fans, but also the whole air duct system. So a fan model and an air duct network model can be added to the natural ventilation model (see annex 5). A heat recovery device can also complete the system.

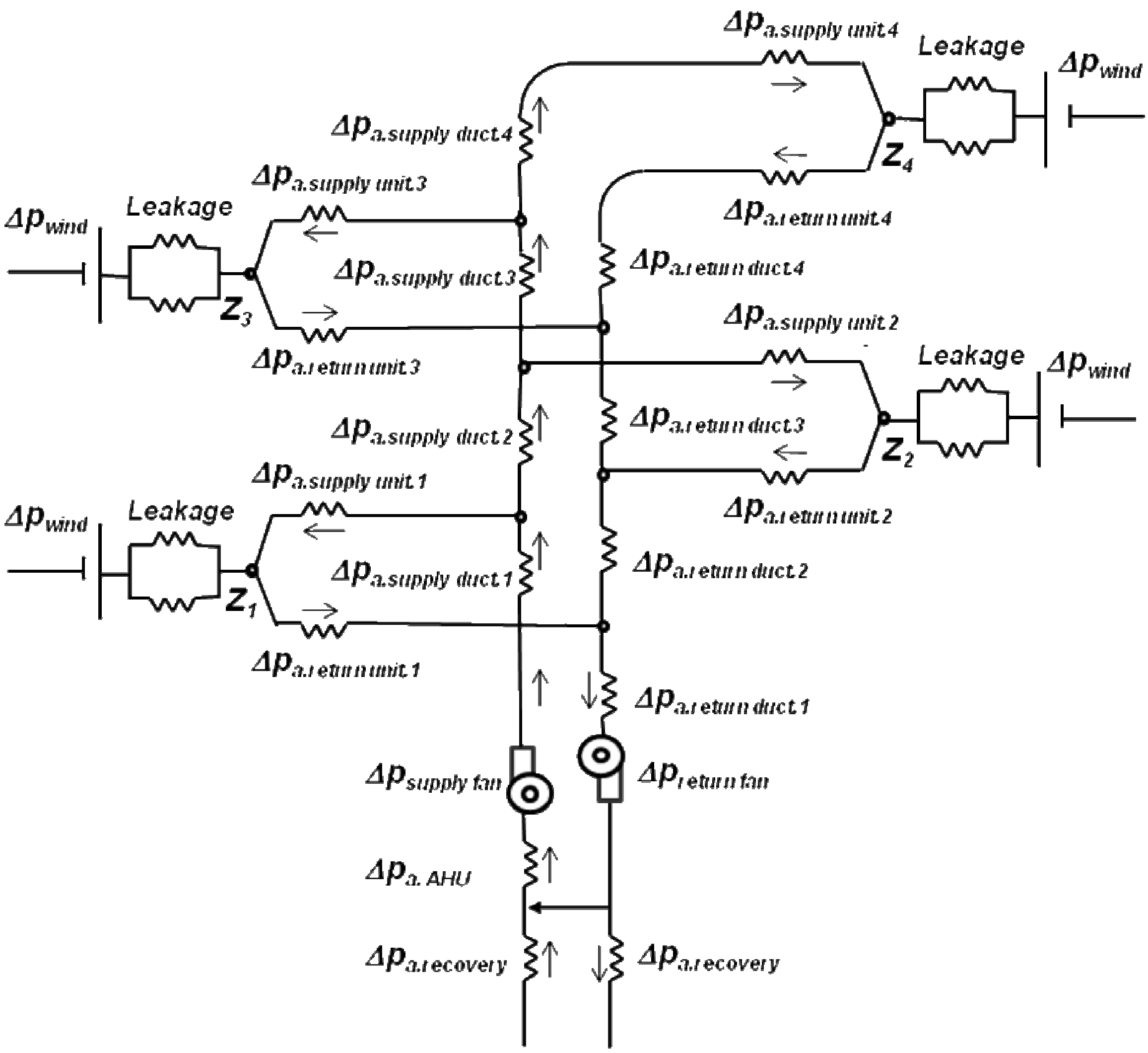

Fig. A 6.7 Combined type D ventilation model including four building zones, supply and return air ducts with the corresponding supply and return fans.

As far as natural ventilation devices are concerned, air leakage can be maintained while Controlled Supply Orifices are removed. The Controlled Exhaust Orifice and the exhaust ventilation shaft can be sized for a reduced air flow rate corresponding to lavatories air exhaust:

$$30\, m^3/h + \mathit{Number\ of\ sanitary\ devices} \,.\, 15\, m^3/h$$

with one sanitary device for 5 occupants.

Type D system model is presented on fig A 6.7. The four offices natural ventilation model of fig. A 6.4 is superimposed to the model of fig. 6.7 (with leakage instead of CSO) in order to build a whole combined ventilation model of type D ventilation system. A heat recovery device and an Air Handling Unit can complete the model.

Equations (A 6.7) to (A 6.9) related to the office natural ventilation are modified to deal with type D ventilation system including supply and return ducts.

Pressure drops:

For each zone: equations (6.12)

For the corridor:

$$\Delta p_{CEO} = K_{ceo} \cdot \dot{M}_{CEO} \cdot \left|\dot{M}_{CEO}\right|^{n_{CEO}}$$

$$\Delta p_{chem} = K_{chem} \cdot \dot{M}_{CEO} \cdot \left|\dot{M}_{CEO}\right|^{n_{CEO}} \qquad \text{(A 6.12)}$$

For the air handling unit:

$$\Delta p_{a,recovery} = f_{a,recovery,ON} \cdot K_{recovery} \cdot \left|\dot{M}_{a,fresh}\right| \cdot \dot{M}_{a,fresh}$$

$$\Delta p_{a,ahu} = K_{AHU} \cdot \left|\dot{M}_{a,supply\,fan}\right| \cdot \dot{M}_{a,supply\,fan} \qquad \text{(A 6.13)}$$

For each air duct slice between two zones:

$$\dot{M}_{a,su,duct} = \sum_{k=zone}^{n_{zones}} \left(\dot{M}_{a,supply,zone,k}\right)$$

$$\Delta p_{a,supply\,duct} = K_{supply\,duct} \cdot \left|\dot{M}_{a,su,duct}\right| \cdot \dot{M}_{a,su,duct} \qquad \text{(A 6.14)}$$

For each zone delivered by an air duct system:

$$\Delta p_{a,supply\,zone} = \sum_{k=1}^{zone} \left(\Delta p_{a,supply\,duct,k}\right) + \Delta p_{a,supply\,unit}$$

$$\Delta p_{a,supply\,unit} = K_{supply\,unit} \cdot \left|\dot{M}_{a,supply,zone}\right| \cdot \dot{M}_{a,supply,zone} \qquad \text{(A 6.15)}$$

Equations (A 6.14 and A 6.15) are written similarly for the the return air duct.

Pressure equilibrium:

For natural ventilation of each zone (fig. A 6.4) with stack effect instead of chimney:

$$-\Delta p_{wind,pr} + \Delta p_{pr} + \Delta p_{TO} - \Delta p_{CEO} + \Delta p_{stack,in} - \Delta p_{stack} - \Delta p_{dz,stack,out} = 0$$

$$-\Delta p_{wind,pr} + \Delta p_{pr} - \Delta p_{pr,dw} + \Delta p_{wind,pr,dw} = 0$$

For fan powered ventilation of each zone (fig. A 6.7):

$$\Delta p_{su} = \Delta p_{a,recovery} + \Delta p_{a,ahu} - \Delta p_{a,supply fan} + \Delta p_{a,supply zone} \quad \text{(A 6.16)}$$

$$\Delta p_{ex} = \Delta p_{a,return zone} + \Delta p_{a,recovery} - \Delta p_{a,return fan}$$

$$\Delta p_{su} + \Delta p_{ex} = 0$$

For fan powered and natural ventilation interaction in each zone (Δp_{pr} through leakage area):

$$\Delta p_{su} - \Delta p_{pr} - \Delta p_{wind,pr} = 0$$

Mass air flow rate balance:

For each zone:

$$\dot{M}_{TO} = \dot{M}_{cso} + \dot{M}_{so,up} + \dot{M}_{so,dw} + \dot{M}_{a,supply,zone} - \dot{M}_{a,return,zone} \quad \text{(A6.17)}$$

For the corridor:

$$\dot{M}_{CEO} + \sum_{j=1}^{n_{zones}} (\dot{M}_{TO}) = 0$$

6.2.2.3. Fan running point

The fan design air flow is equal to the sum of the nominal air flows corresponding to the delivered offices. The fan can be sized for that given design air flow $\dot{V}$ and for a given pressure delivered by the fan Δp_{total} compensating the maximum friction loss occurring when air is supplied to (or returned from) the different offices. Maximum friction loss generally occurs for the farthest delivered office.

For given α_i coefficients, a fan rotation speed *N* and a fan diameter *D* can be adopted provided an optimal flow factor ϕ and an associated pressure factor ψ are given (annex 5):

$$D = \left(\frac{4.\dot{V}}{\pi^2 \phi}\right)^{0.5} \Big/ \left(\frac{2.v.\Delta p_{tot}}{\pi^2 \psi}\right)^{0.25} \qquad N = \left(\frac{2.v.\Delta p_{tot}}{\pi^2 \psi}\right)^{0.75} \Big/ \left(\frac{4.\dot{V}}{\pi^2 \phi}\right)^{0.5} \qquad \text{(A 6.18)}$$

For the supply fan, pressures drops occur in the recovery device, the AHU unit and the ducts, while for the return fan they only occur in the recovery device and in the ducts:

$$\Delta p_{a,supply\,fan,n} = \Delta p_{a,recovery,n} + \Delta p_{a,ahu,n} + \Delta p_{a,supply\,zone,n}$$
$$\Delta p_{a,return\,fan,n} = \Delta p_{a,recovery,n} + \Delta p_{a,return\,zone,n} \qquad \text{(A 6.19)}$$

In OFF DESIGN conditions, the location of the fan running point is variable. For a given fan rotation speed, the fan running point depends on fan and building pressure/ air flow rate laws.

Fan model equations (chapter 5) provide a relationship between *fan air flow rate* and *total fan pressure increase*, for a given fan rotation speed.

For given wind speed and associated pressure coefficients, and for given outdoor/indoor temperatures, the ventilation model (§6.2.2.1 and 6.2.2.2) provide other relationships between *building and air ducts ventilation air flow rates* and *pressure drops* in the building natural ventilation devices, as well as in the duct network leading to the farthest office. They can be merged with fan model equations in order to find the fan running point for a given fan rotation speed. The fan total pressure increase as well as the fan air flow rates can be deduced from the location of that fan running point.

The pressure delivered by the supply fan $\Delta p_{a,supply\ fan}$ as well as the volume air flows supplied by the fan $\dot{V}_{a,supply\ fan}$ are thus resulting from a global pressure balance including fan pressure increases, air ducts pressure losses and building natural ventilation devices pressure drops.

The total fan supplied mass air flow is:

$$\dot{M}_{a,supply\,duct} = \dot{M}_{a,supply,zone,1} \qquad \text{(A 6.20)}$$

The total pressure increase of the supply fan $\Delta p_{a,supply\ fan}$ *is:*

$$\Delta p_{a,supply\,zone,4} = \sum_{k=1}^{n_{zones}} \left(\Delta p_{a,supply\,duct,k} \right) + \Delta p_{a,supply\,unit,4}$$

For the *air return duct* and for the *return fan,* equations can be developed similarly. So, the total pressure delivered by the fans $\Delta p_{a,supply\ fan}$, $\Delta p_{a,return\ fan}$ as well as the fan air flow rates $\dot{V}_{a,supply\ fan}$, $\dot{V}_{a,return\ fan}$ can be deduced.

6.2.2.4. Air ducts modelling

This section is meant to express the *straight duct* and *local friction coefficients K*, defined in chapter 6 §6.1, as function of the duct air flow rate, so that starting from the *K* coefficient related to the main duct, coefficients related to other duct slices can be deduced as function of the ratio of air flow rates.

Air ducts can be sized according to the *constant friction method*: the friction loss in a straight duct is constant in each duct slice.

The main duct deserving the total design air flow rate $\dot{V}_{a,tot,n}$ can then be sized for a given air speed $u_{a,duct}$:

$$\dot{V}_{a,tot,n} = \sum_{j=1}^{n_{zones}} \left(\dot{V}_{a,n,j} \right) \qquad d_{duct} = \left[4 \cdot \frac{\dot{V}_{a,tot,n}}{u_{a,duct} \cdot \pi} \right]^{0.5} \qquad \text{(A 6.21)}$$

The corresponding *straight duct friction loss* $\Delta p_{lin,duct}$ can be deduced, provided a duct roughness ε_{duct} is given as model parameter [32]:

$$\Delta p_{lin,duct} = \frac{\lambda \cdot u_{a,duct}^{\ 2}}{2 \cdot d_{duct} \cdot v_n} \qquad Re = u_{a,duct} \cdot \frac{d_{duct}}{\nu_n} \qquad \text{(A 6.22)}$$

$$\lambda = \frac{1}{\left[2 \cdot \mathbf{log} \left(\frac{2.51}{Re \cdot \lambda^{0.5}} + \frac{\varepsilon_{duct}}{d_{duct} \cdot 3.71} \right) \right]^2}$$

$$\nu_n = \frac{14}{10^6} \cdot 1 \quad [m^2/s] \qquad \varepsilon_{duct} = \frac{0.15}{10^3} \cdot 1 \quad [m]$$

Finally, a straight duct friction coefficient, named $K_{lin,duct}$, can be computed for that main duct (see *K* definition in chapter 1, §1.1):

$$K_{lin,duct} = \frac{\Delta p_{lin,duct}}{\dot{M}_{a,tot,n}^{\ 2}} \qquad \dot{M}_{a,tot,n} = \frac{\dot{V}_{a,tot,n}}{v_n} \tag{A 6.23}$$

As all air ducts are assumed to be sized according to a *constant friction method*, the straight duct friction loss $\Delta p_{lin,duct}$ is the same for all of them. From (A6.23), each duct slice friction coefficient $K_{lin,i}$ is proportional to *1/(air flow rate)*^{2}.

Starting from the main duct straight friction loss coefficient $K_{lin,duct}$, the straight friction loss coefficients $K_{lin,i}$ corresponding to duct slice *i*, conveying air flow rate $\dot{V}_i$, can be expressed as:

$$\frac{K_{lin,i}}{K_{lin,duct}} = \left(\frac{\dot{V}_{a,tot,n}}{\dot{V}_{a,i}}\right)^2 \quad \text{or} \quad \frac{K_{lin,i}}{K_{lin,i+1}} = \left(\frac{\dot{V}_{a,i+1}}{\dot{V}_{a,i}}\right)^2 \tag{A 6.24}$$

Local friction losses occur when *diversions* or *confluences* exist (Fig. A 6.8).

Fig. A 6.8: Diversion (left) and confluence (right) in an air duct network.

The local pressure drop is given by:

$$\Delta p_{loc} = \zeta . \frac{u_{a,duct}^{\ 2}}{2.v} \tag{A 6.25}$$

Factor ζ is related to the ratio of air speeds after and before the diversion or confluence. For a straight air flow, the ζ_1 factor related to the air speed u_1 can be expressed as function of the air speed ratio $u_{2/}\, u_1$ (Fig. A 6.8 and ref [32]):

$$\textit{Diversion:} \quad \zeta_1 = 1 - \left(\frac{u_2}{u_1}\right)^2 \tag{A 6.26}$$

$$\textit{Confluence:} \quad \zeta_1 = 1{,}6.\left(1 - \left(\frac{u_2}{u_1}\right)^2\right)$$

A local friction *K* coefficient named $K_{loc,1}$ can be computed from (A 6.23) and (A 6.25):

$$\Delta p_{loc} = \zeta_1 . \frac{u_1^{\ 2}}{2.v} = K_{loc,1} . \dot{M}_{a,1}^2 = K_{loc,1} . \frac{u_1^{\ 2}}{v^2} . \left(\frac{\pi . d_1^2}{4}\right)^2$$

$$K_{loc,1} = 8.\zeta_1 . \frac{v}{\pi^2 . d_1^4} \tag{A 6.27}$$

The local friction coefficient is proportional to $\zeta/(diameter)^4$ (A 6.27).

Starting from the local friction coefficient $K_{loc,i}$ related to the duct i, the local friction coefficients $K_{loc,i+1}$ related to duct i+1 can be written:

$$\frac{K_{loc,i+1}}{K_{loc,i}} = \frac{\zeta_{i+1}}{\zeta_i} \cdot \left(\frac{d_i}{d_{i+1}}\right)^4 \qquad \text{(A 6.28)}$$

That expression includes a ratio of diameters and a ratio of ζ factors. Both ratios can be expressed as function of the ratio of air flow rates.

Assuming a turbulent air flow and smooth air ducts, the friction coefficient λ is proportional to $Re^{-0,25}$ [32]. So the friction coefficient λ is proportional to $(u_{a,duct} \cdot d_{duct})^{-0,25}$ (A6.22).

As all air ducts are sized according to a *constant friction method*, the straight duct friction loss $\Delta p_{lin,duct}$ is the same for all of them, with $\Delta p_{lin,duct}$ proportional to $\lambda . u^2_{a,duct} / d_{duct}$ (A6.22).

So, in a first approximation, $\lambda . u^2_{a,duct} / d_{duct}$ can be considered as constant for the different duct slices, and $u^7_{a,duct} / d^5_{duct}$ can be considered as constant too:

$$\left(\frac{u_{i+1}}{u_i}\right)^7 = \left(\frac{d_{i+1}}{d_i}\right)^5 \qquad \text{(A 6.29)}$$

As the air speed $u_{a,duct}$ is proportional to the ratio $\dot{V}_{a,duct}/d^2_{duct}$, where $\dot{V}_{a,duct}$ is the duct air flow rate, the ratio $\dot{V}^7_{a,duct}/d^{19}_{duct}$ can be assumed constant the different duct slices.

Finally, the diameters ratio appearing in (A 6.28) can be expressed:

$$\left(\frac{d_i}{d_{i+1}}\right)^4 = \left(\frac{\dot{V}_i}{\dot{V}_{i+1}}\right)^{28/19} \qquad \text{(A 6.30)}$$

The ratio of ζ factors appearing in (A 6.28) can also be expressed as function of the ratio of air flow rates.

Factor ζ_1 is a function of $(u_2/u_1)^2$ (A 6.26). Equations (A 6.29) and (A 6.30) can give:

$$\left(\frac{u_2}{u_1}\right)^2 = \left(\frac{d_2}{d_1}\right)^{10/7} = \left(\frac{\dot{V}_2}{\dot{V}_1}\right)^{10/19} \qquad \text{(A 6.31)}$$

Local friction losses can be expressed as function of the ratio of entering and leaving air speeds for a diversion (or of the ratio of leaving and entering speeds for a confluence), with can itself be expressed as function of the air flow rates ratio ((A 6.26),(A 6.28), (A 6.30) and (A 6.31)):

$$\frac{K_{loc,i+1}}{K_{loc,i}} = \frac{\zeta_{i+1}}{\zeta_i}\left(\frac{\dot{V}_{i-1}}{\dot{V}_i}\right)^{\frac{28}{19}} = \left(\frac{\dot{V}_i^{\frac{10}{19}}-\dot{V}_{i+1}^{\frac{10}{19}}}{\dot{V}_{i-1}^{\frac{10}{19}}-\dot{V}_i^{\frac{10}{19}}}\right)\left(\frac{\dot{V}_{i-1}}{\dot{V}_i}\right)^2 \qquad \text{(A 6.32)}$$

Starting from the main duct local friction loss coefficient for a straight air flow $K_{loc,duct}$, the local friction loss coefficients $K_{loc,i}$ corresponding to the different duct slices i, conveying air flow rates $\dot{V}_i$, can be computed.

6.2.2.5. Network pressure balance

The design pressure drop can be computed as the maximum friction loss occurring when air is supplied to (or returned from) the different offices. It generally occurs for the farthest delivered office.

The pressure drop occurring in each duct slice in nominal conditions can be computed by:

$$\Delta p_{a,supply\,duct,n} = K_{supply\,duct} \cdot \left|\dot{M}_{a,su,duct,n}\right| \cdot \dot{M}_{a,su,duct,n} \qquad \text{(A 6.33)}$$

The maximum pressure drop can be computed for the farthest office delivered by the air duct, including the pressure drop occurring in its supply unit:

$$\Delta p_{a,supply\,zone,n,4} = \sum_{k=1}^{n_{zones}} \left(\Delta p_{a,supply\,duct,n,k}\right) + \Delta p_{a,supply\,unit,n,4}$$

The *network pressure balance* can then be performed by adapting the friction loss K coefficient of offices air supply units, in order to reach the design pressure drop for each office deserving network branch:

(A 6.34)

$$K_{supply\,unit} \cdot \dot{M}_{a,supply,zone,n}^{\;2} = \Delta p_{a,supply\,zone,n,4} - \sum_{k=1}^{zone} \left(\Delta p_{a,supply\,duct,k}\right)$$

A similar process can be used to perform the return duct network balance.

ANNEX 7: AIR QUALITY ANALYSIS

7.1. House air quality analysis

The ground floor (zone 1) can be occupied during the day from 7 AM to 11 PM, while the first floor (zone 2) can be occupied during the night from 10 PM to 7 AM (Fig A 7.1). Zone 1 can be heated at 22°C by radiators during the occupancy, while zone 2 can only be maintained at a minimum 10°C temperature.

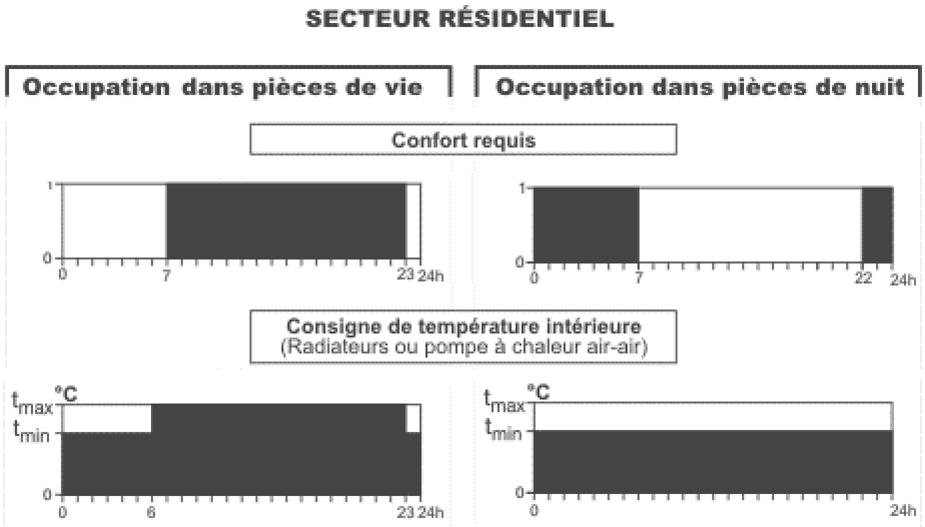

Fig. A 7.1: Seneffe house occupancy profiles

ANNEX 8: SUMMER COMFORT ANALYSIS

8.1. House summer comfort analysis

The ground floor (zone 1) can be occupied during the day from 7 AM to 11 PM, while the first floor (zone 2) can be occupied from 4 PM to 8 AM (Fig A 8.1).

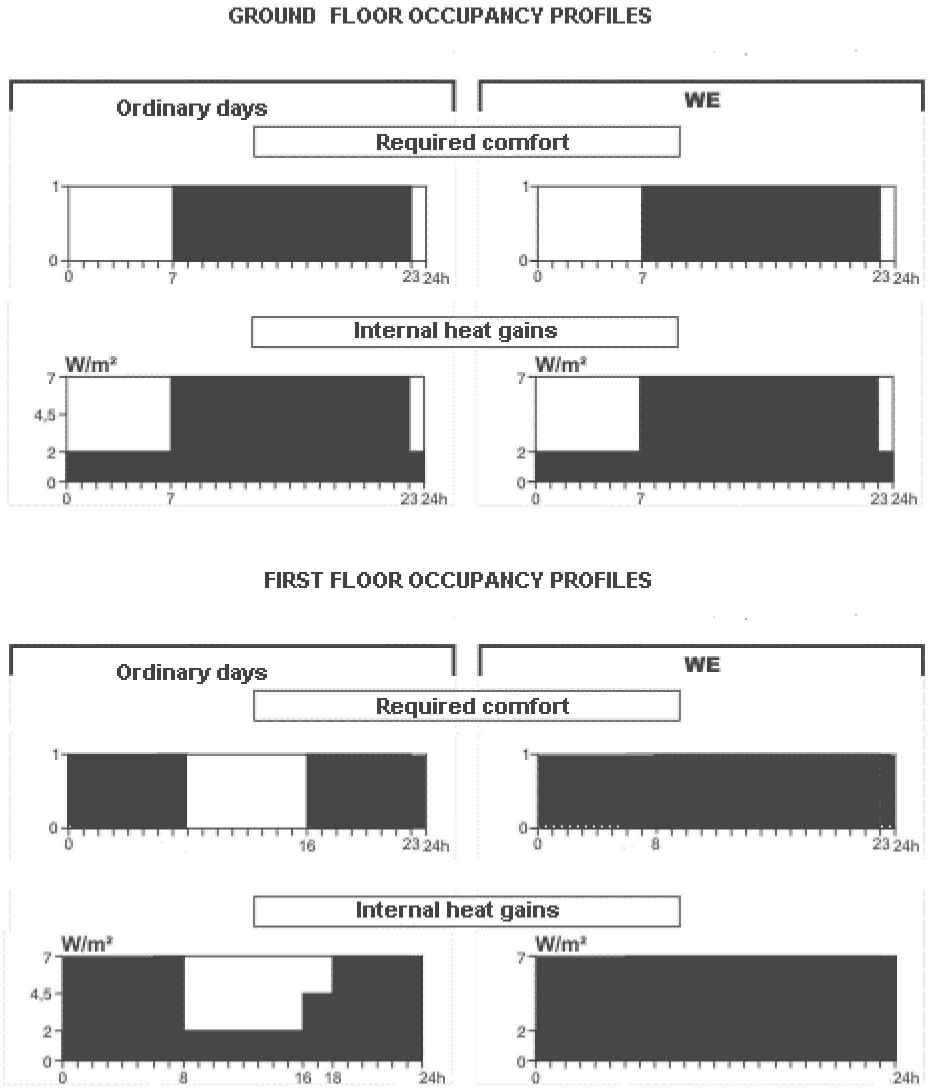

Fig. A 8.1 Occupancy profiles for ground floor and first floor of Esneux house.

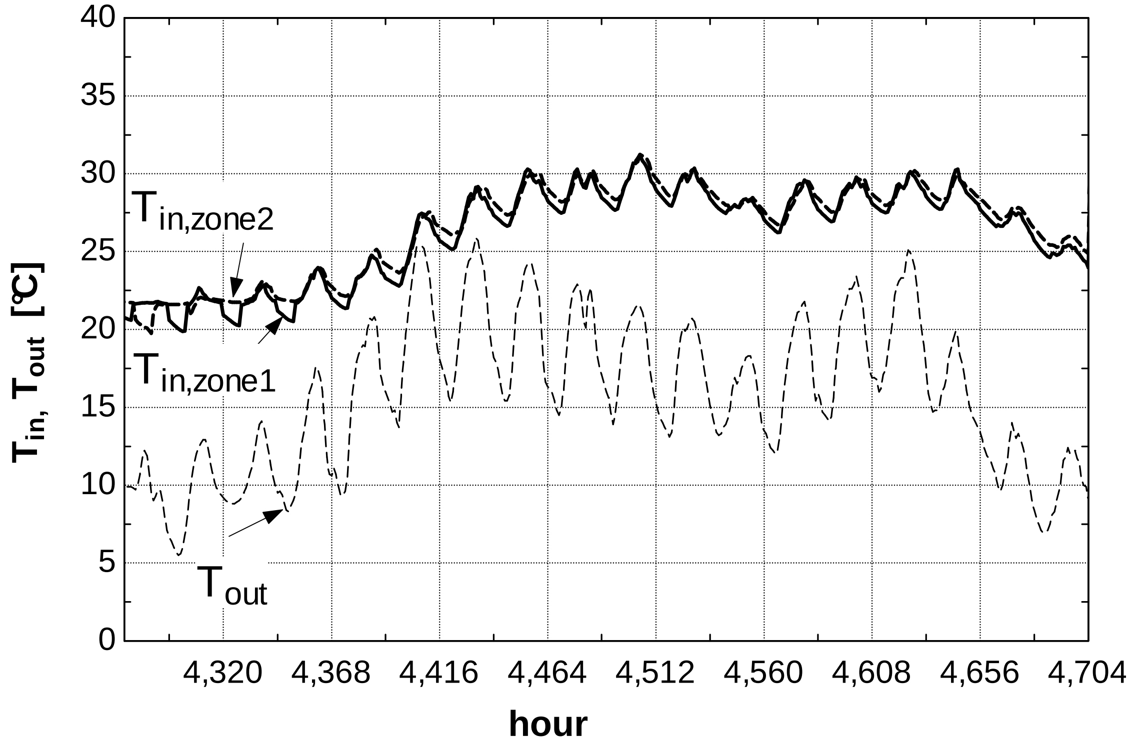

Fig. A 8.2: Indoor temperatures computed in both Esneux house zones, with corresponding outdoor temperatures, for a mean summer, without comfort improvement strategies.

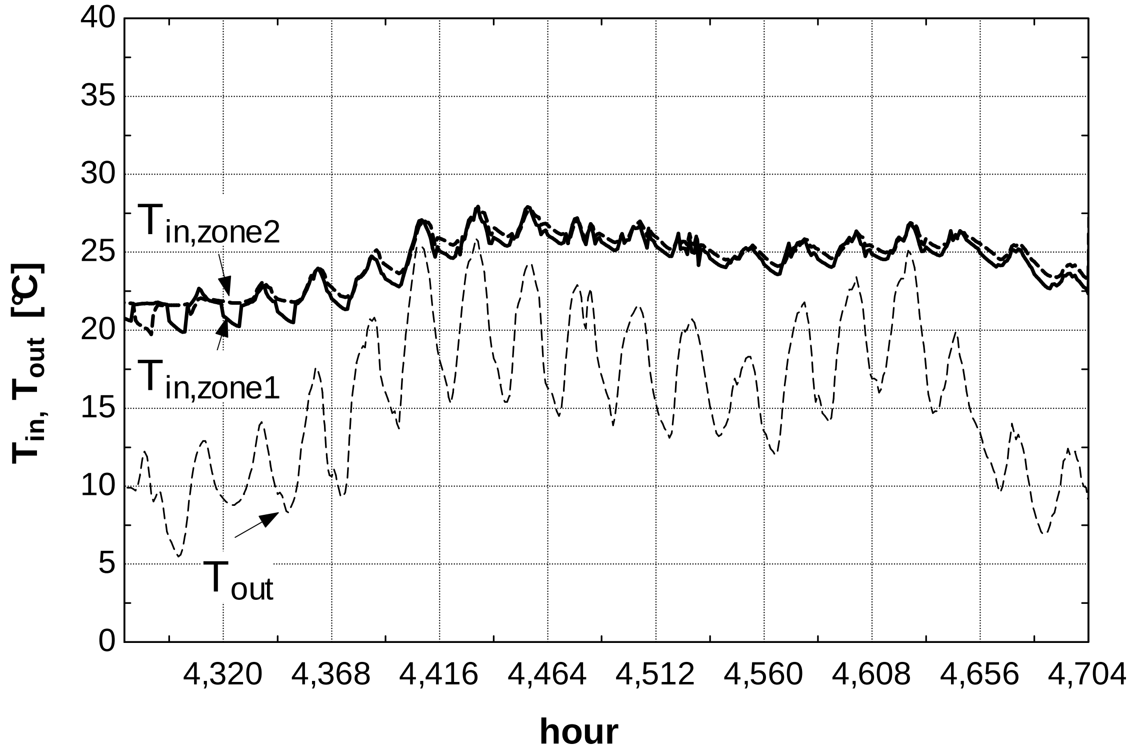

Fig. A 8.3 Indoor temperatures computed in both Esneux house zones, with corresponding outdoor temperatures, for a mean summer, with free-cooling.

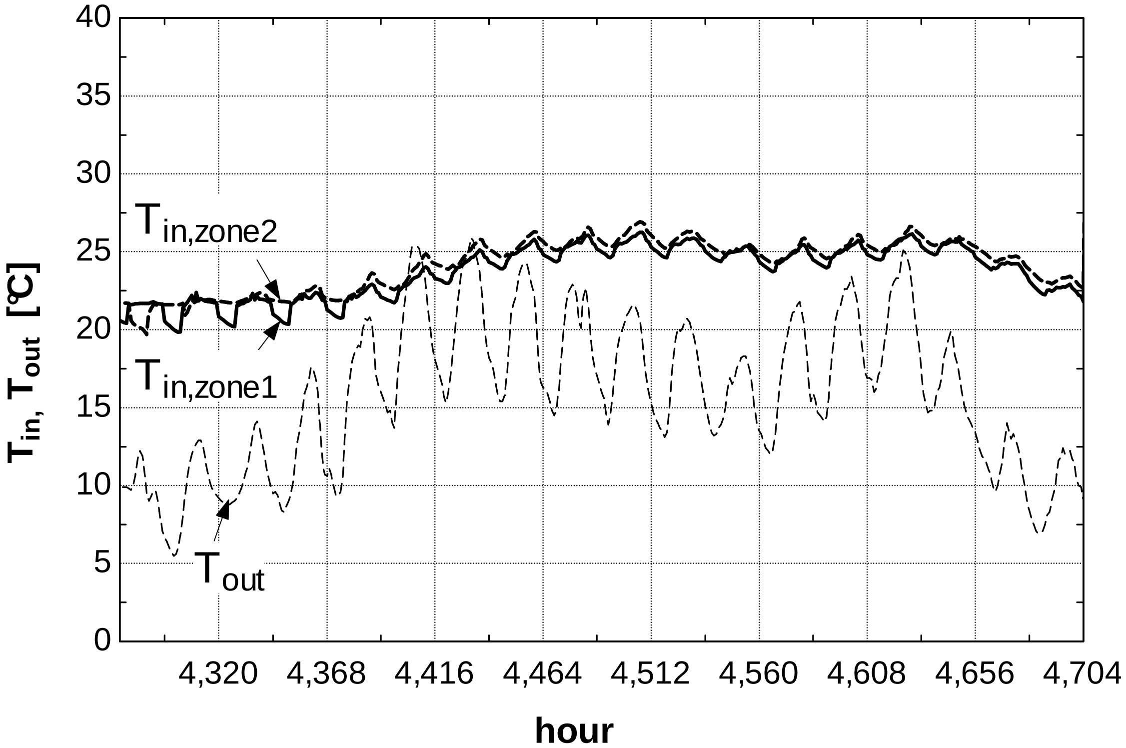

Fig. A 8.4 Indoor temperatures computed in both Esneux house zones, with corresponding outdoor temperatures, for a mean summer, with controlled external blinds.

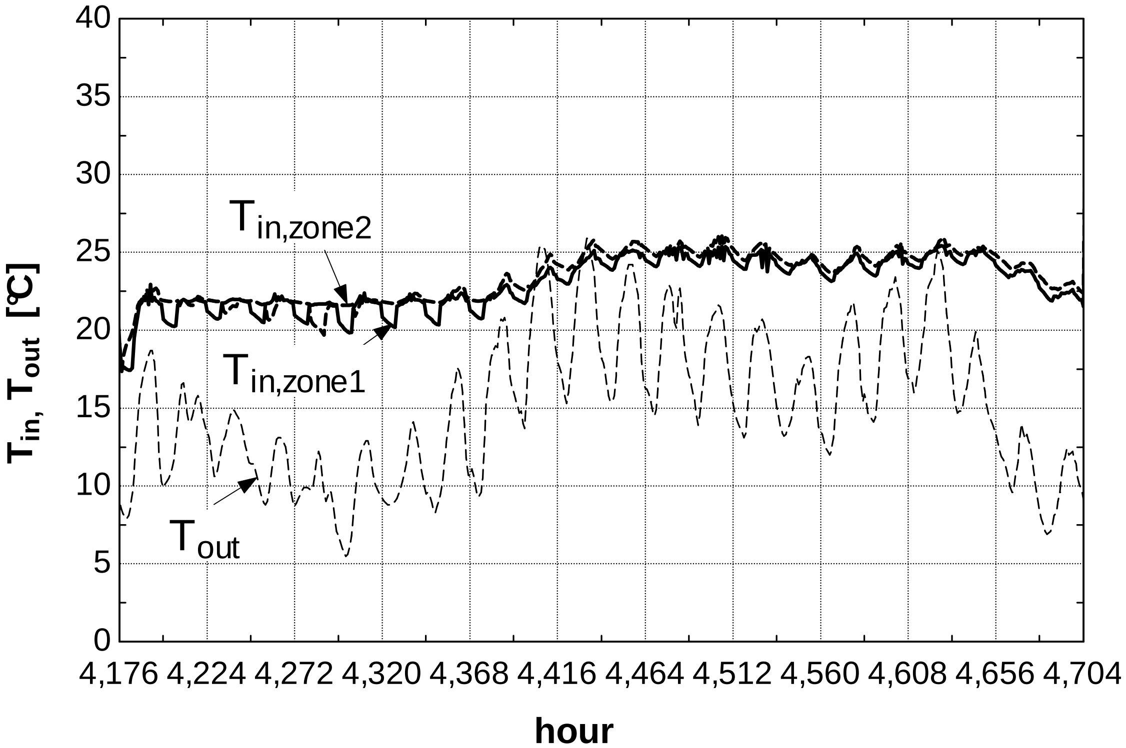

Fig. A 8.5 Indoor temperatures computed in both Esneux house zones, with corresponding outdoor temperatures, for a mean summer, with controlled external blinds and free cooling.

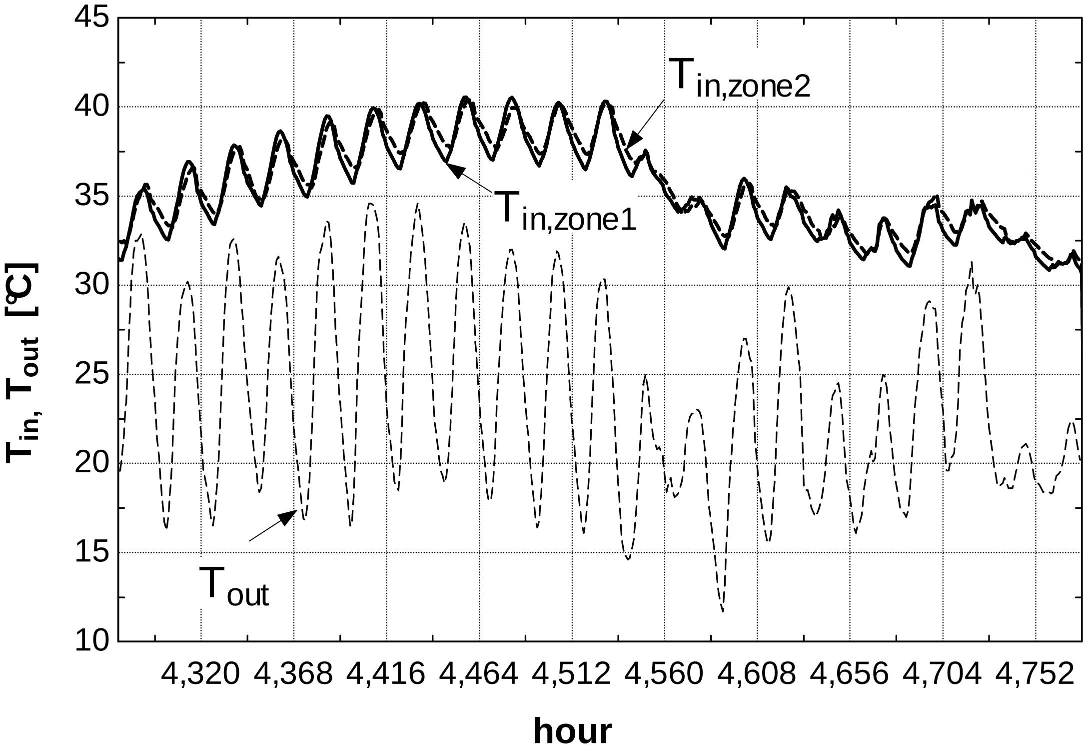

Fig. A 8.6 Indoor temperatures computed in both Esneux house zones, with corresponding outdoor temperatures, for 1976 summer hot wave, without comfort improvement strategies.

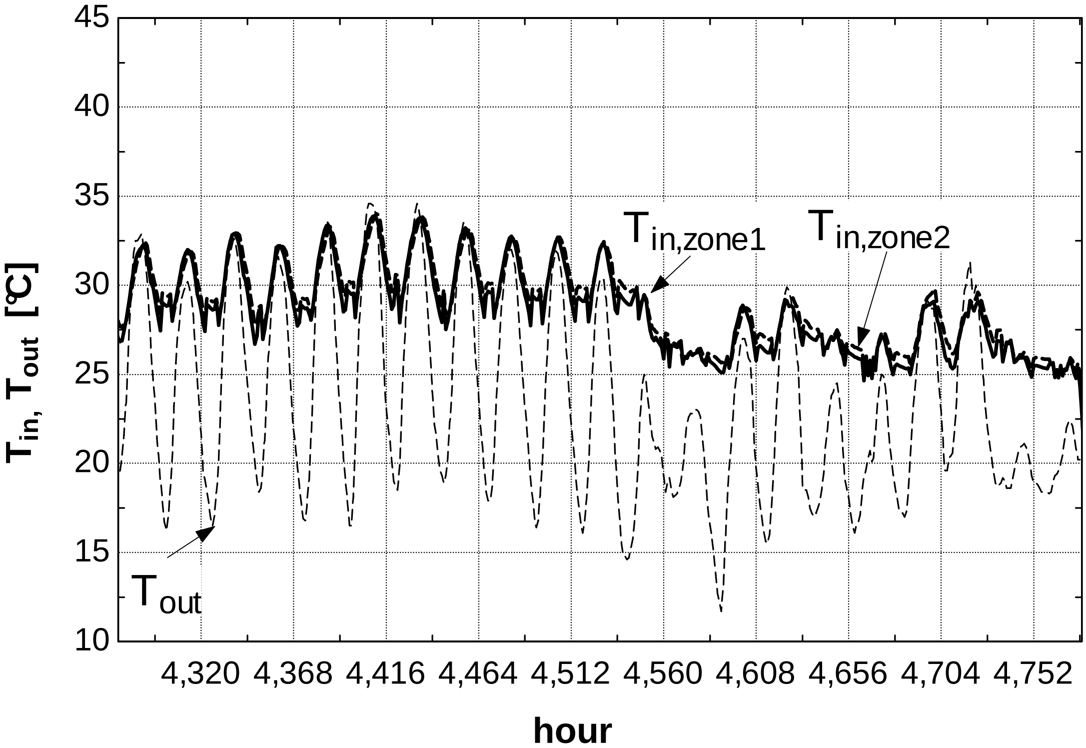

Fig.A 8.7 Indoor temperatures computed in both Esneux house zones, with corresponding outdoor temperatures, for 1976 summer hot wave, with free-cooling.

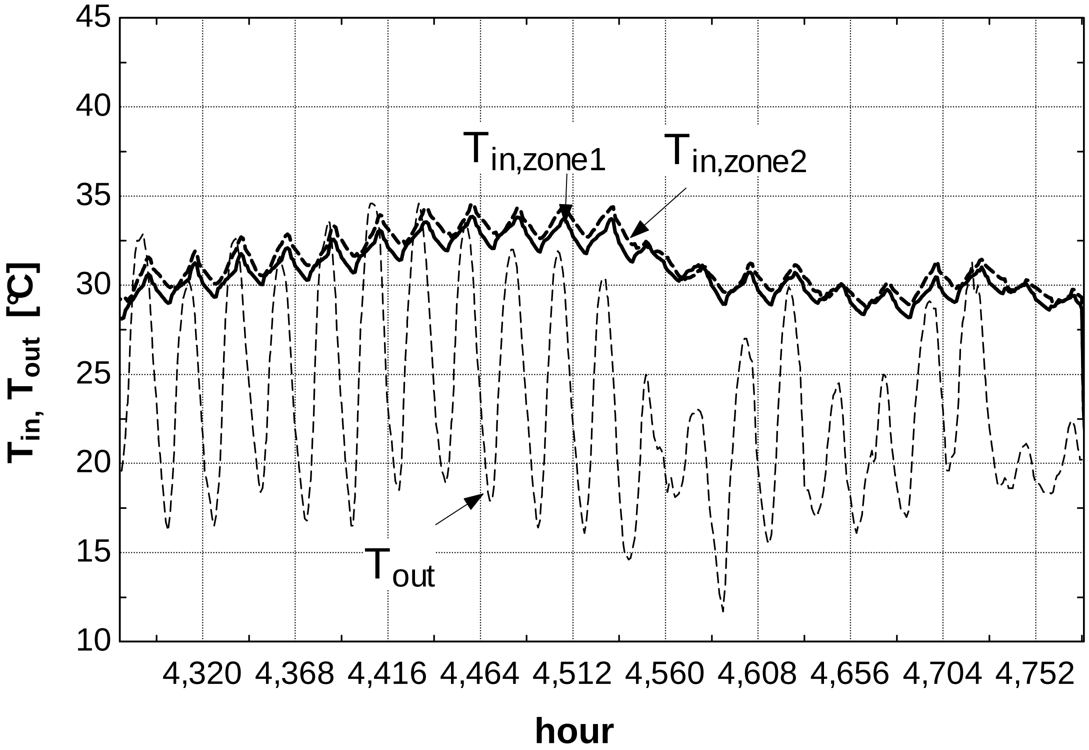

Fig.A 8.8 Indoor temperatures computed in both Esneux house zones, with corresponding outdoor temperatures, for 1976 summer hot wave, with external blinds.

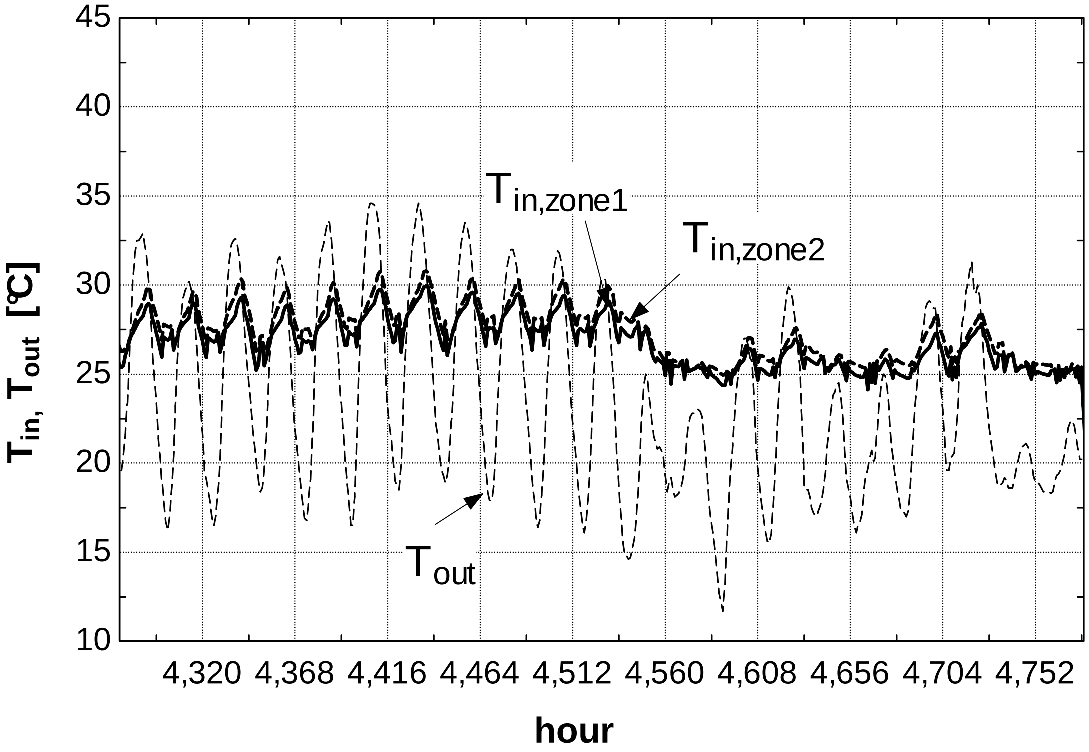

Fig. A 8.9 Indoor temperatures computed in both Esneux house zones, with corresponding outdoor temperatures, for 1976 summer hot wave, with external blinds and free-cooling.

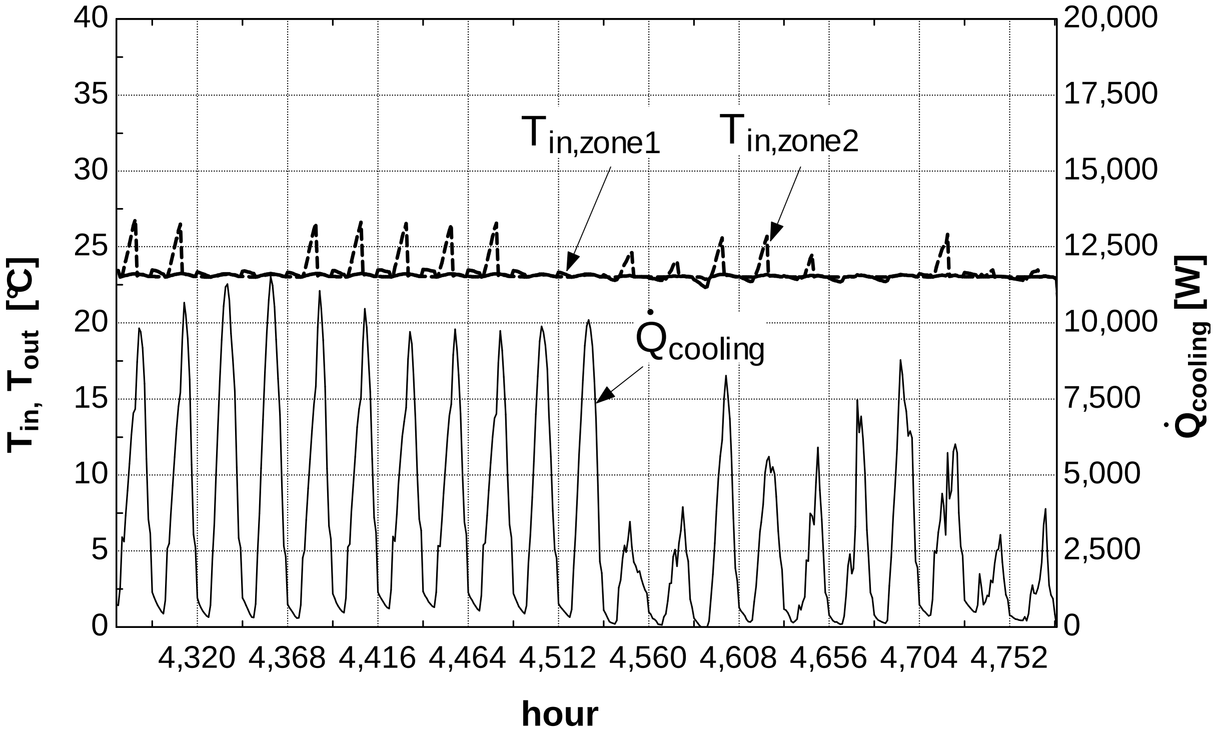

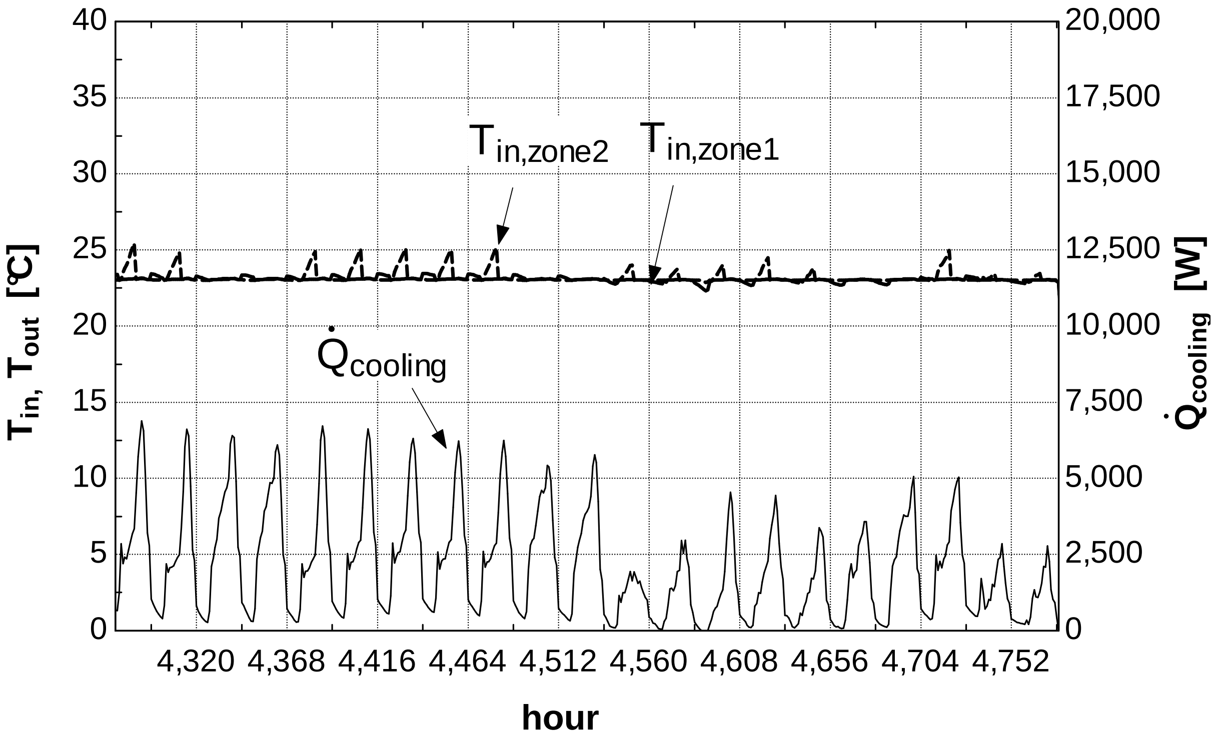

Fig. A 8.10 Indoor temperatures computed in both Esneux house zones and total cooling demand, for 1976 summer hot wave, using room air conditioners with free cooling only (up) or with free cooling in association with controlled blinds (down).

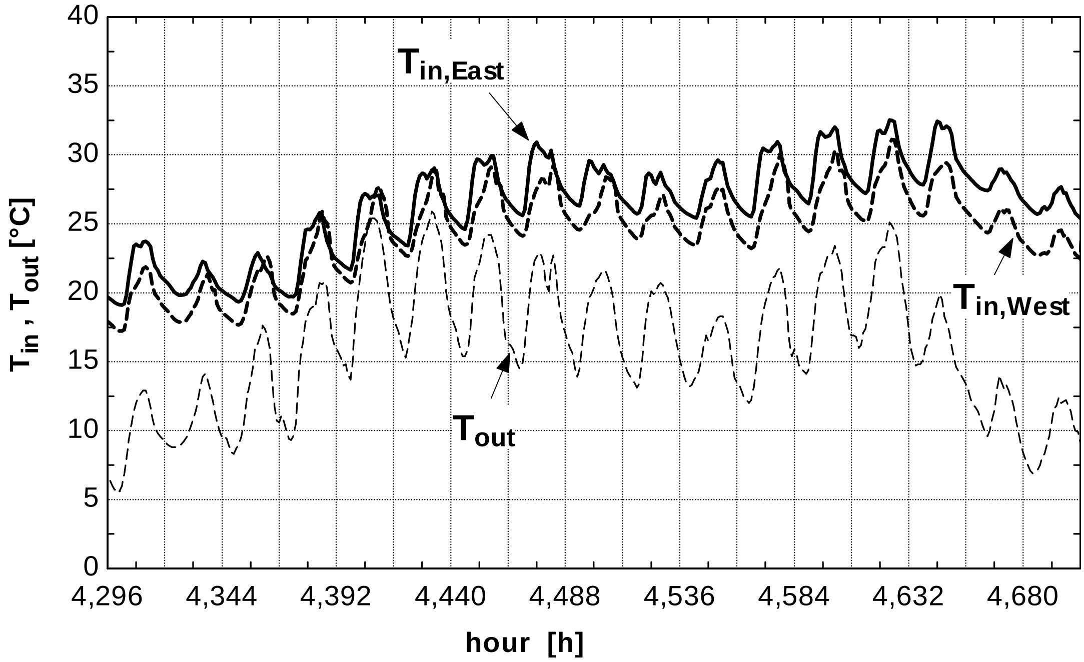

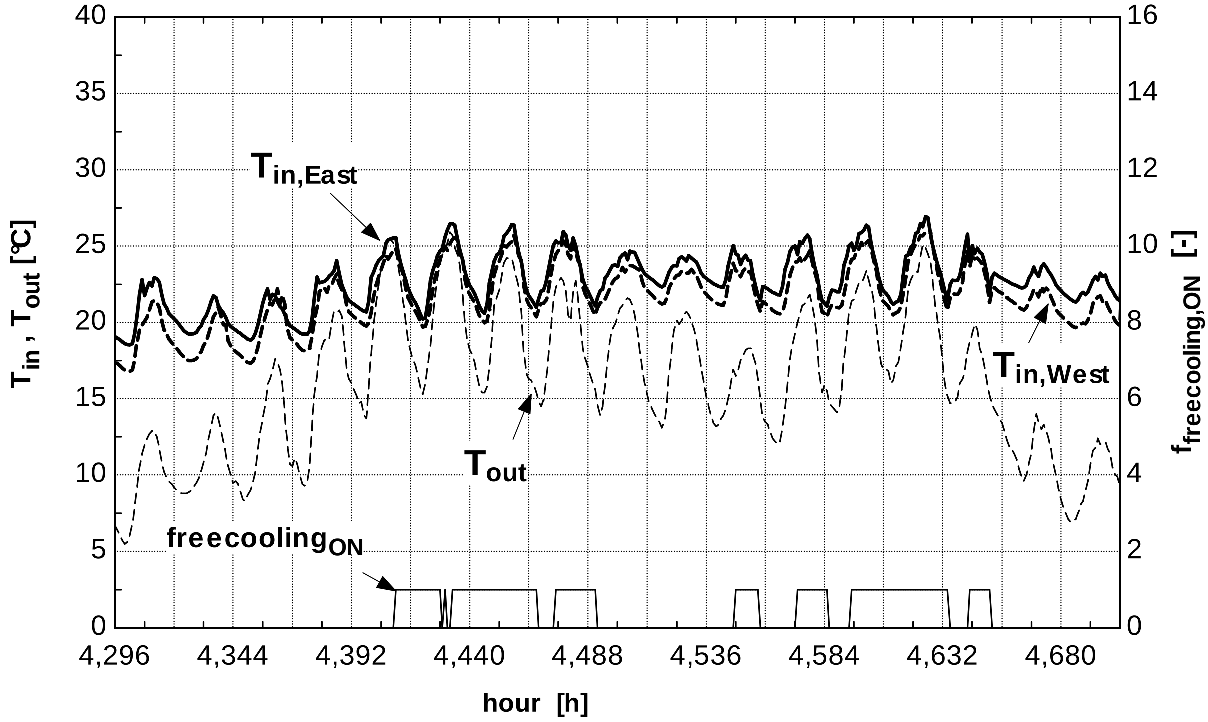

*Fig.A 8.11 Indoor temperatures computed in the East and West fourth floor offices, and corresponding outdoor temperatures, for an **average summer**, without comfort improvement strategy (up) and with room free-cooling and controlled blinds (down).*

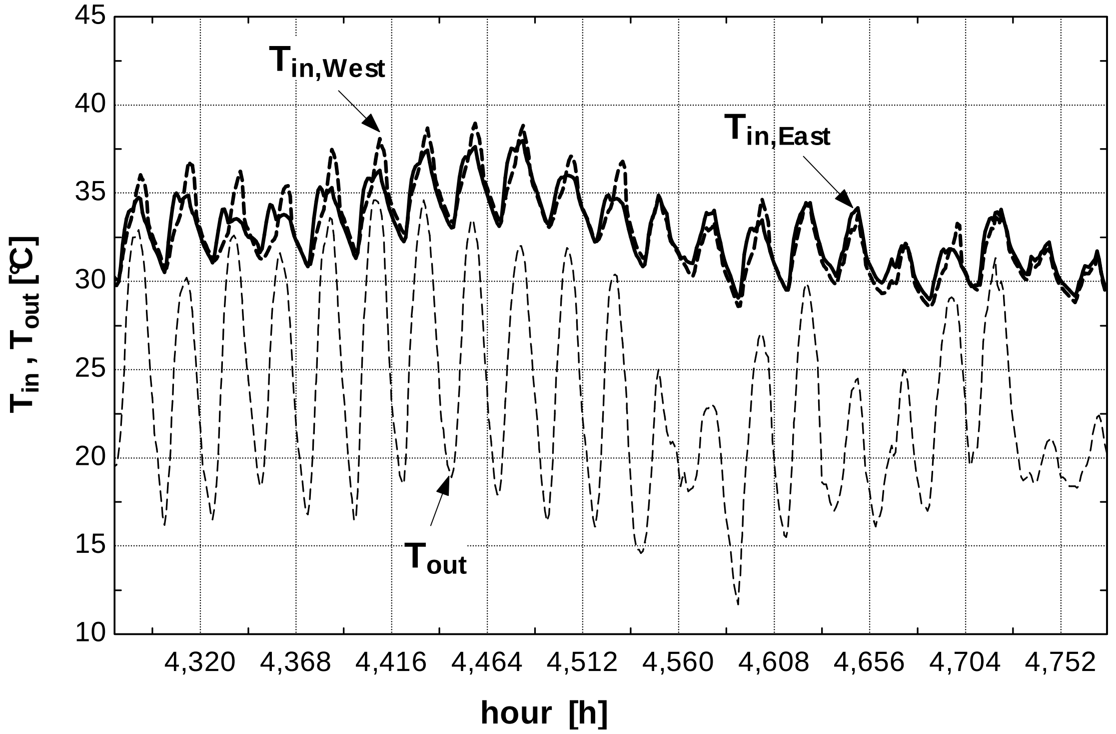

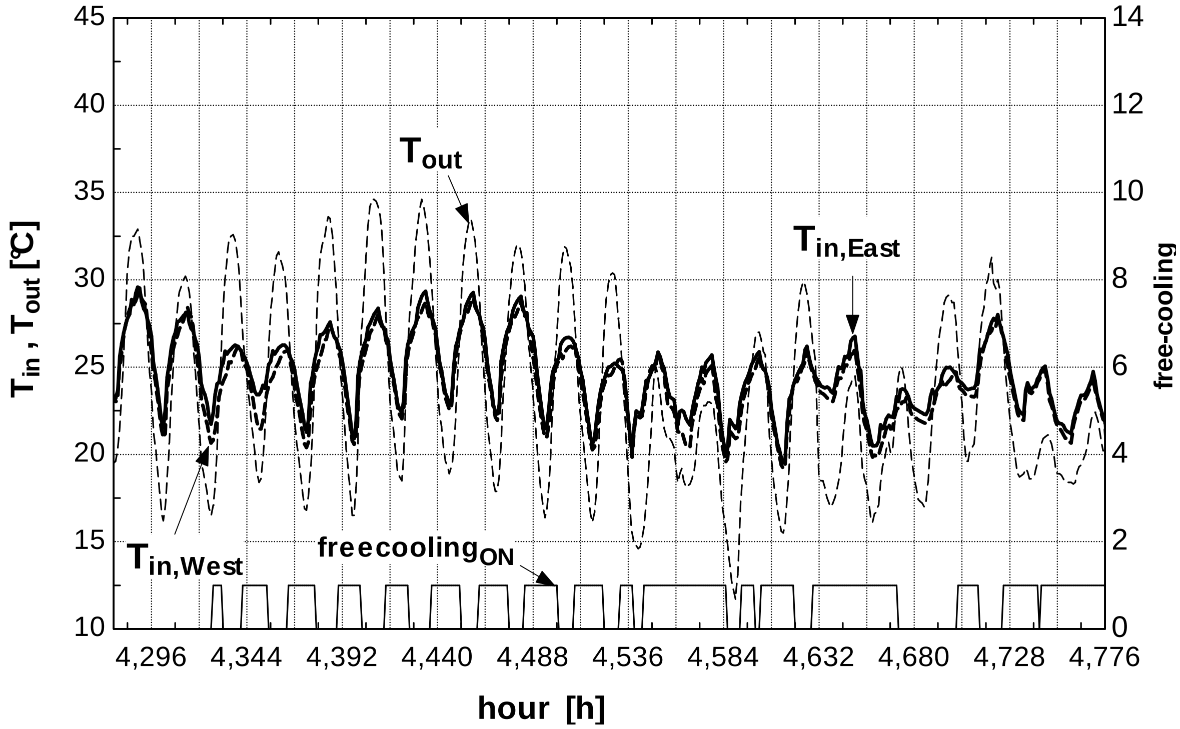

*Fig. A 8.12 Indoor temperatures computed in the East and West ground floor offices, and corresponding outdoor temperatures, for a summer **hot wave**, without comfort improvement strategy (up) and with stack free-cooling and controlled blinds (down).*

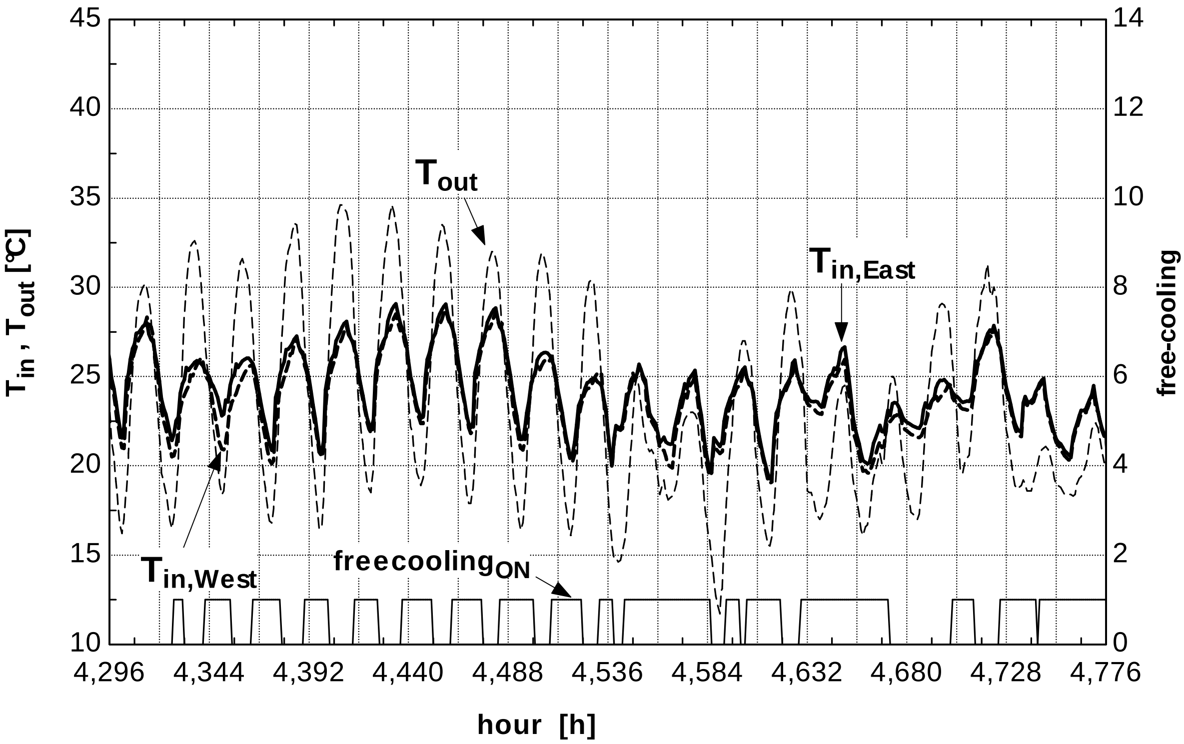

*Fig. A 8.13 Indoor temperatures computed in the East and West ground floor offices, and corresponding outdoor temperatures, for a summer **hot wave**, with type C free-cooling and controlled blinds.*

ANNEX 9: PSYCHROMETRICS

Thermodynamic wet-bulb temperature can be correlated to saturation humidity ratio throught the following equation, valid for a normal pressure of 101325 Pa:

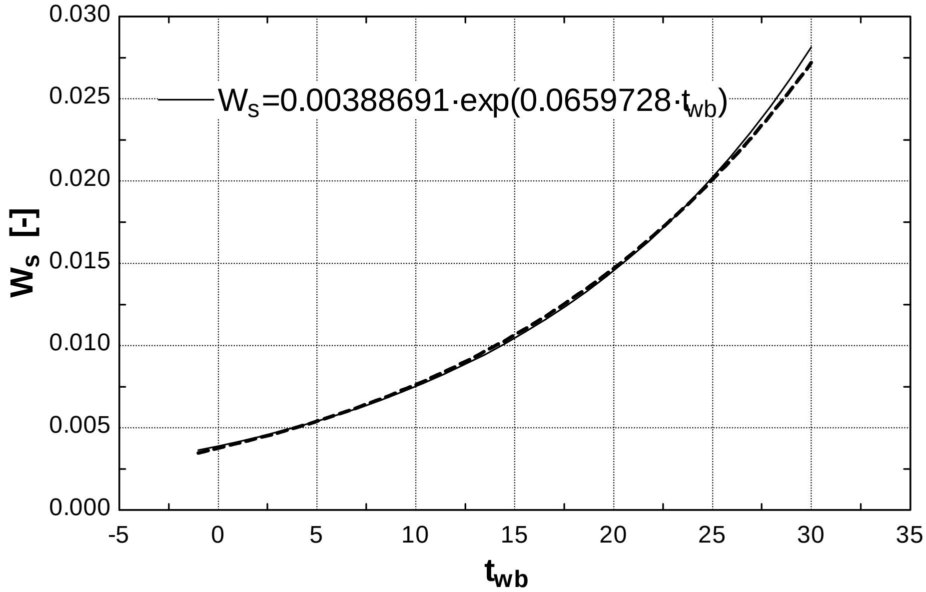

Fig A6.1: Regression curve corresponding to saturation humidity ratio as function of wet-bulb temperature at normal pressure of 101325 Pa.

Thermodynamic wet-bulb temperature can also be correlated to saturation enthalpy throught the following equation, valid for a normal pressure of 101325 Pa:

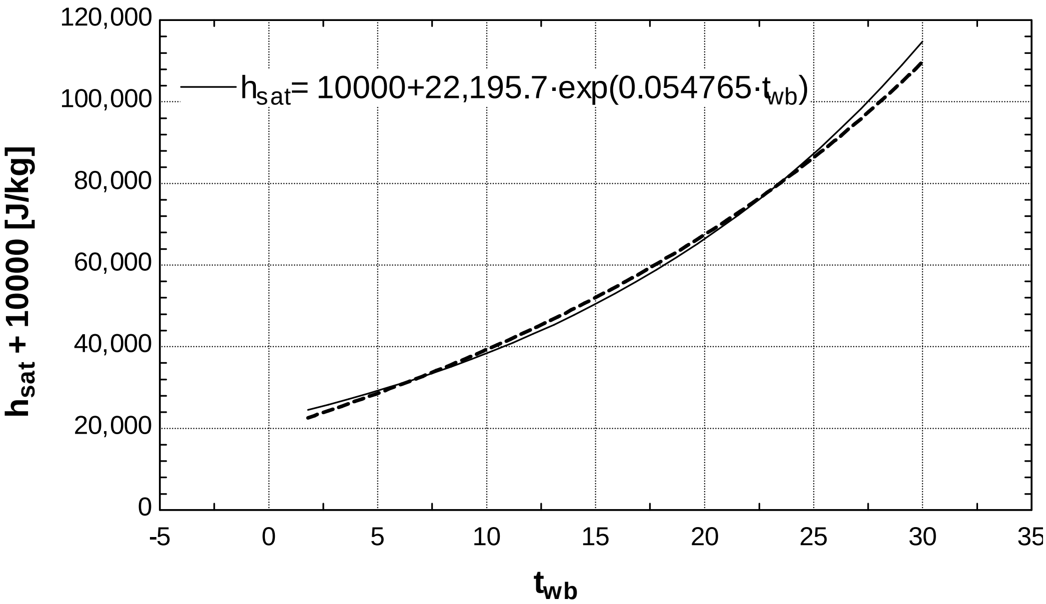

Fig A6.2: Regression curve corresponding to saturation enthalpy as function of air wet-bulb temperature at normal pressure of 101325 Pa.

The *saturated specific heat* of wet cooling coil ficticious saturated air layer, named $c_{p,sat}$ expressed in *J/kg-K,* can be defined as:

$$c_{p,sat} = \frac{h_{a,sat,su,coolingcoil} - h_{a,sat,ex,coolingcoil}}{t_{wb,su,coolingcoil} - t_{wb,ex,coolingcoil}}$$

In that expression, enthalpies correspond to saturated air at supply and exhaust wet-bulb temperatures.

The *saturated specific heat* of wet cooling coil ficticious saturated air layer can be correlated to air supply wet-bulb temperature and to air wet-bulb temperature decrease, through the following equations:

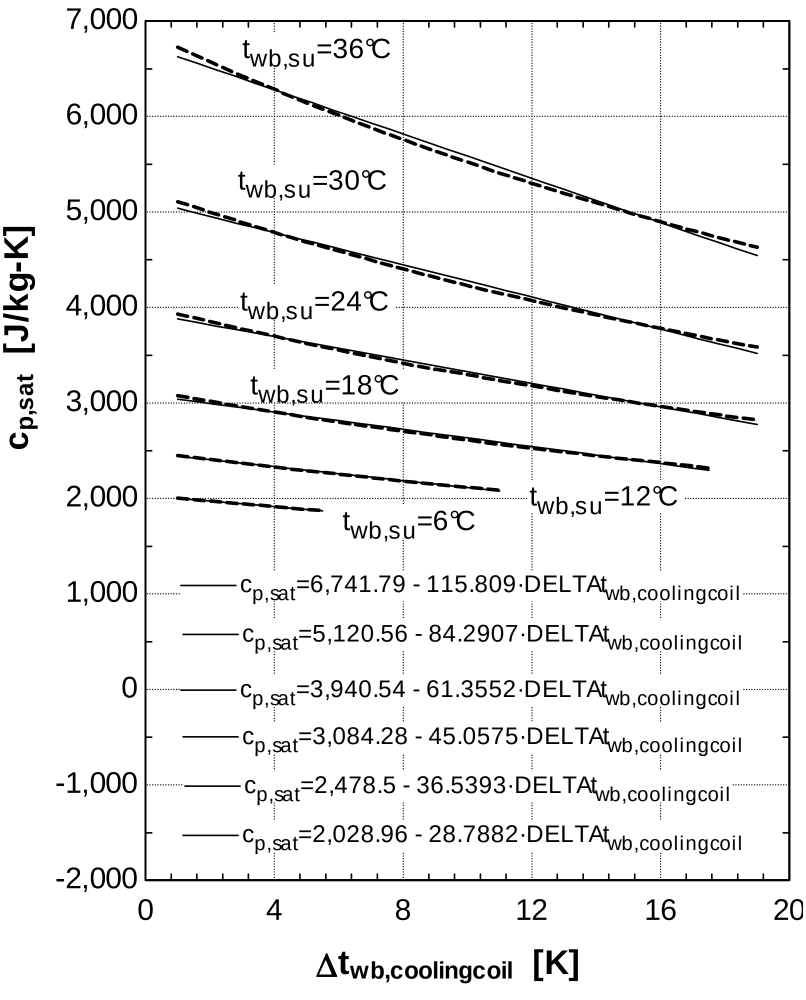

Fig A6.3: Regression curve corresponding to wet cooling coil ficticious saturated air layer specific heat as function of the supply air wet-bulb temperature and of the air wet-bulb temperature decrease, for a normal pressure of 101325 Pa.

Those equations can be written as:

$$c_{p,sat} = a_{coolingcoil} \cdot \Delta t_{wb,coolingcoil} + b_{coolingcoil}$$

The coefficients $a_{coolingcoil}$ and $b_{coolingcoil}$ can be obtained through the following regressions as function of air supply wet-bulb temperature:

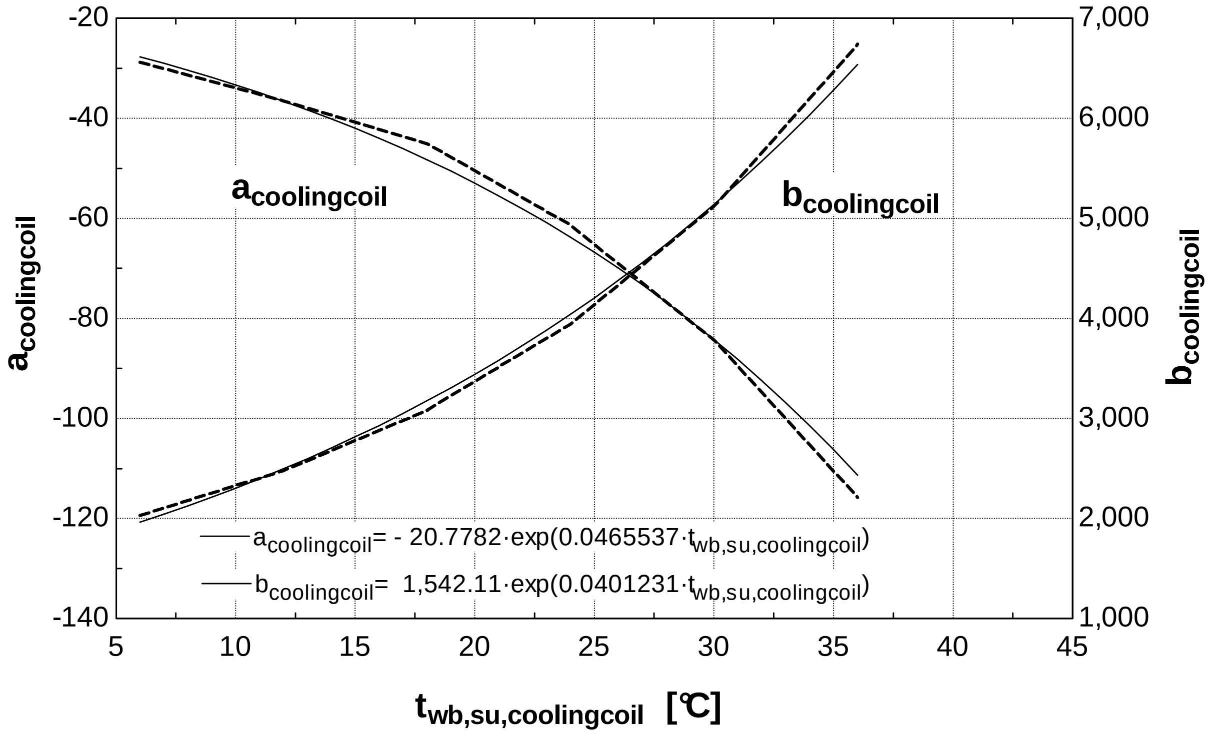

Fig A6.4: Regression curves corresponding to a and b coolingcoil saturated air layer specific heat coefficients, at normal pressure of 101325 Pa.